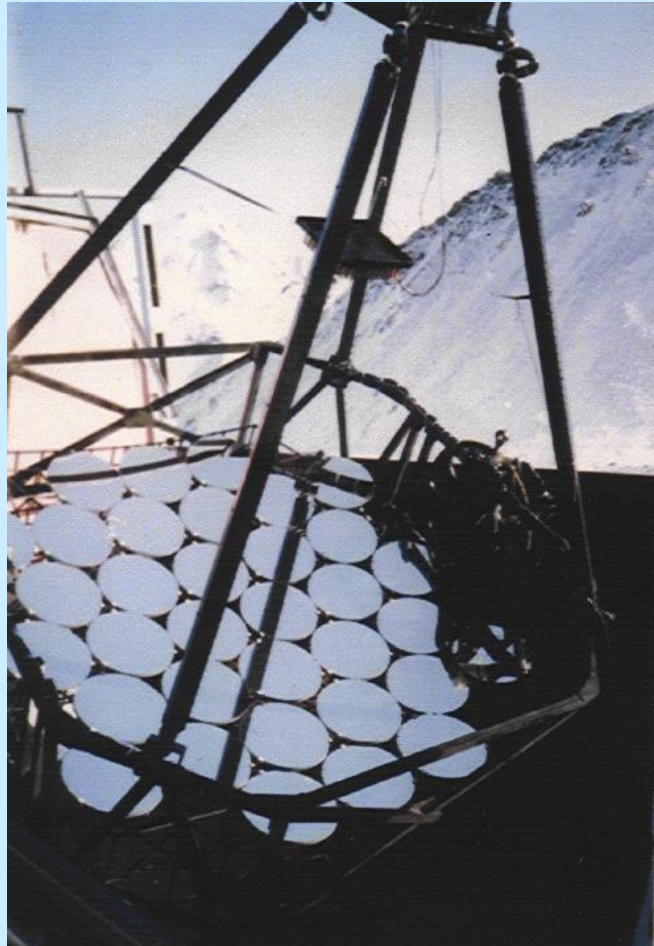


# Very High Energy Astrophysics with the SHALON Cherenkov Telescopes

V.G. Sinitsyna<sup>1</sup> , V.Yu. Sinitsyna<sup>1</sup> , S.S. Borisov<sup>1</sup>,  
A.I. Klimov<sup>1,2</sup>, R. M. Mirzafatikhov <sup>1</sup>, N.I. Moseiko<sup>1,2</sup>

<sup>1</sup> *P.N. Lebedev Physical Institute, RAS*

<sup>2</sup> *NRC«Kurchatov Institute»*

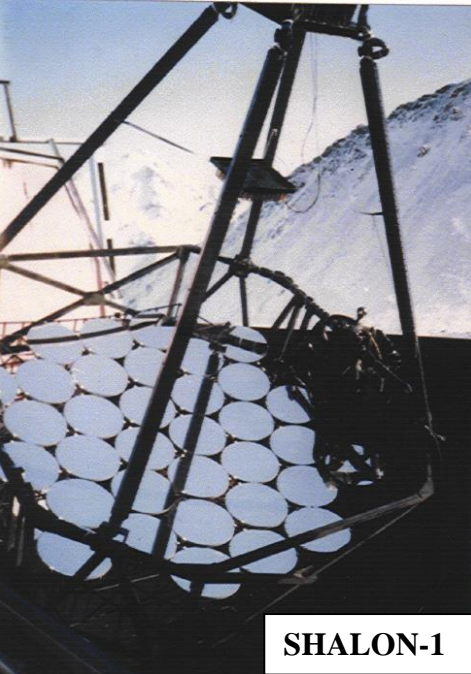


# SHALON Cherenkov Telescopes

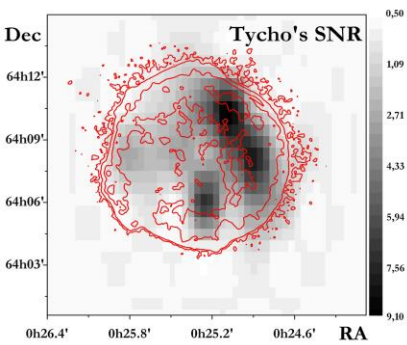
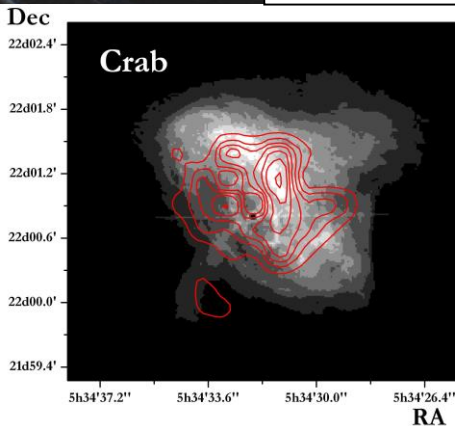
Cherenkov light emission is widely used in numerous astroparticle physics experiments. The success was reached with the detection technique using the imaging atmospheric Cherenkov telescopes. The base of such experiments is that the Cherenkov light emitted from the particles of extensive air shower created by the primary gamma-ray is collected by a mirror reflector and then detected by a pixelized PMT camera.

SHALON are the imaging atmospheric Cherenkov telescopes creating in the P.N. Lebedev Physical Institute for gamma-ray astronomy at the energies of 800 GeV to 100 TeV. It is located in the Tien-Shan mountains at the altitude of 3340 m a.s.l. The telescopic systems have characteristics sufficient to record precise information about the shower structure in this energy range. The idea of enhancement of angular resolution and sensitivity to the  $\gamma$ -rays was realized in SHALON telescopes by the number of technical solutions presented here, including the construction the widest field of view in the world of  $> 8^\circ$ . It allows to enlarge the experiment effective area  $> 10^5 \text{ m}^2$ , then to detect the weak gamma-ray fluxes  $\leq 10^{-13} \text{ cm}^{-2} \text{ s}^{-1}$  due to the high 99.93% rejection of background of cosmic rays and to reconstruct the source structure on the scales  $\sim 20''$  as a result of the better determination of the gamma-ray arrival direction.

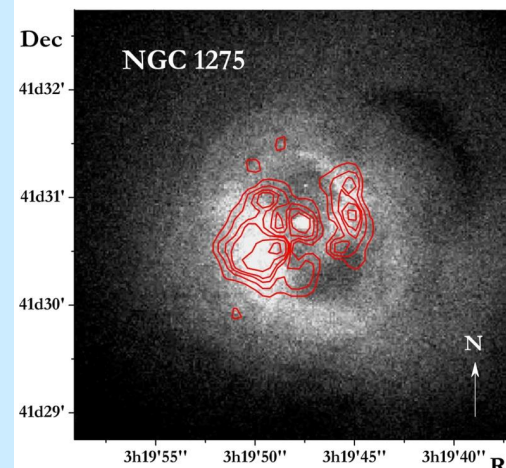
- SHALON experiment has been operating since 1992 and covers the wide astroparticle physics topics including an acceleration and origin of cosmic rays in supernova remnants, the physics of relativistic flaring objects like a black holes and active galactic nuclei as well as the long-term studies of the different type objects.



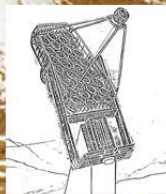
SHALON-1



SHALON-2



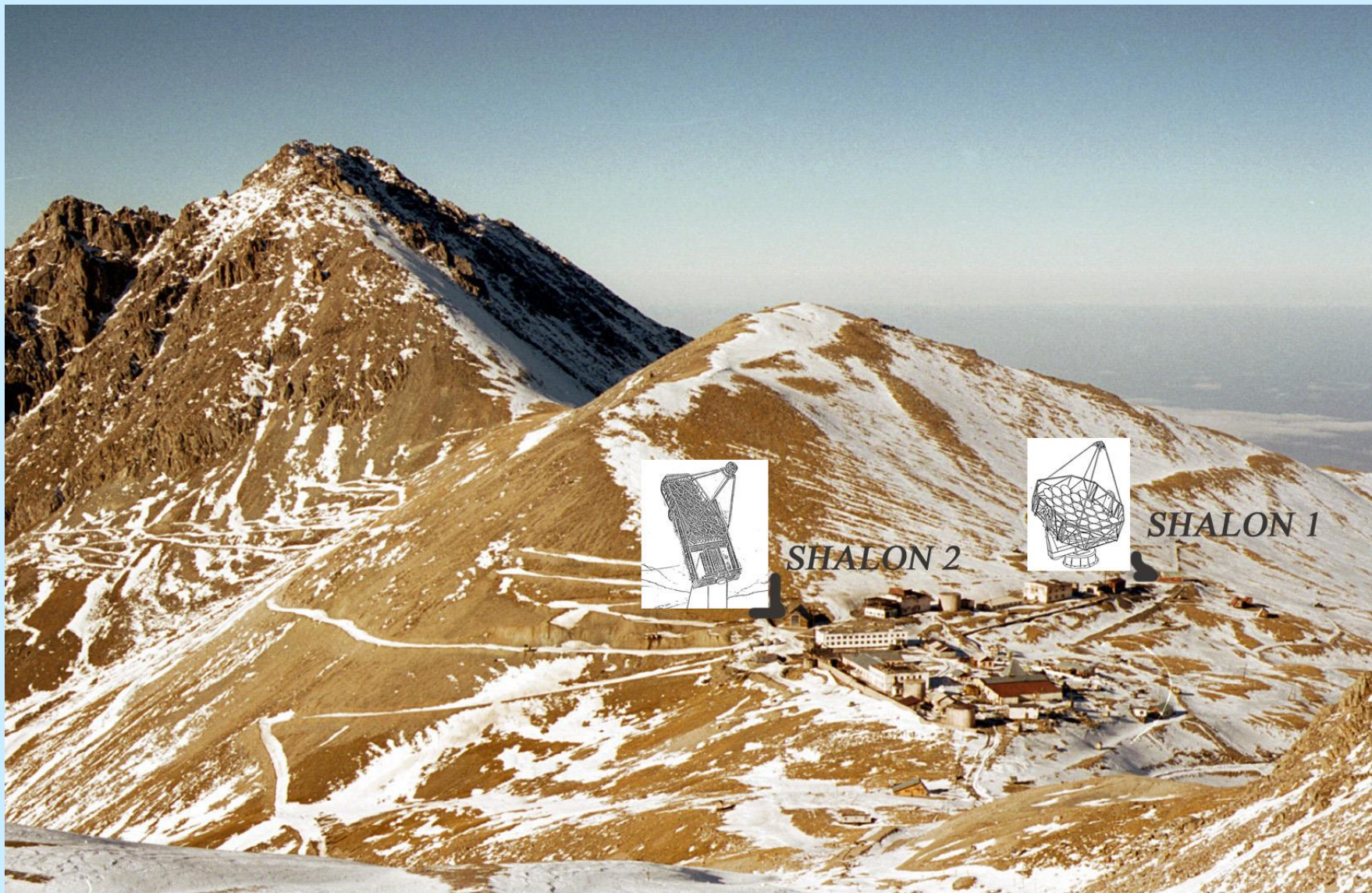




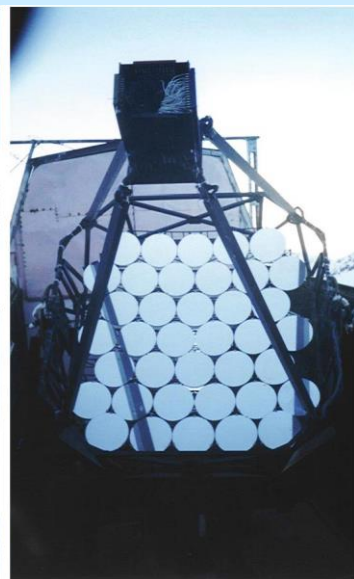
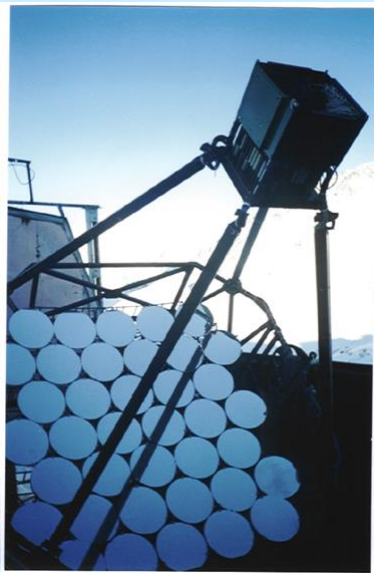
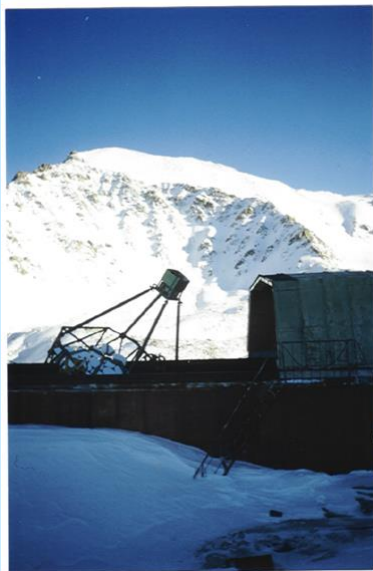
SHALON 2



SHALON 1







SHALON-1

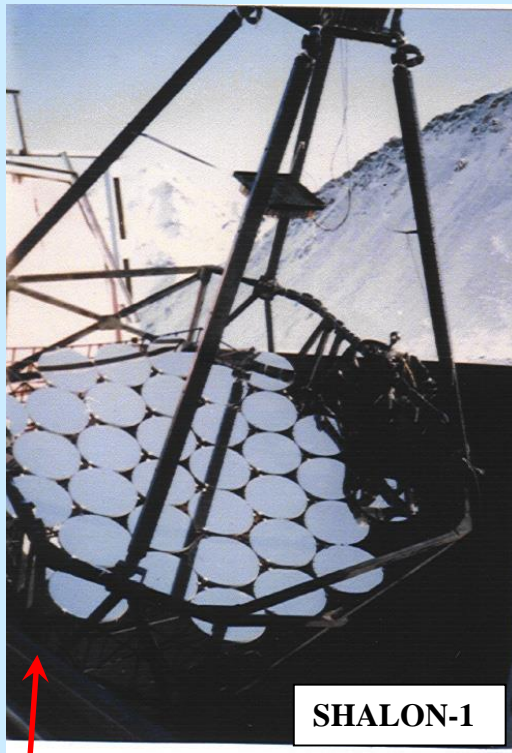


SHALON-2

# SHALON OBSERVATORY

for 800 GeV – 100 TeV gamma-astronomy

SHALON mirror Cherenkov telescope created in 1992

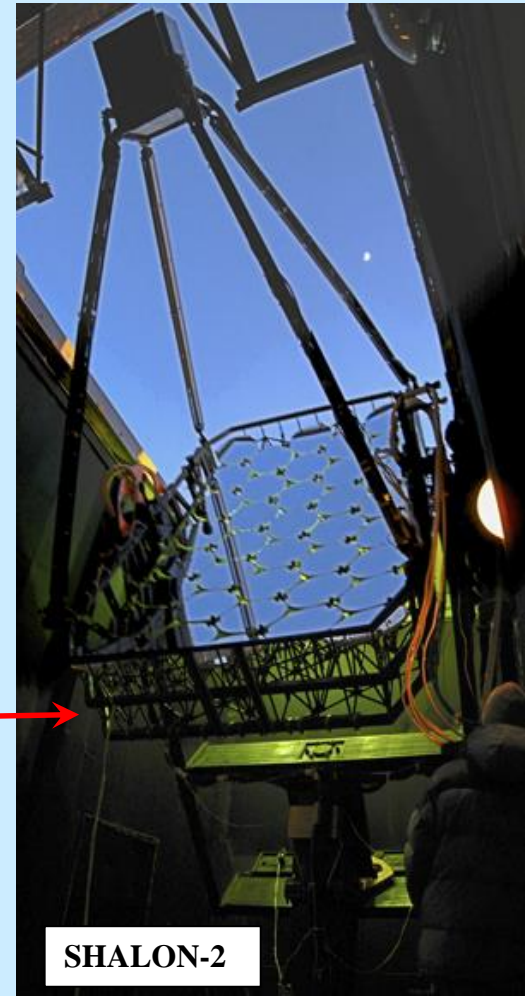


- The size of the composed spherical mirror -  $11.2 \text{ m}^2$
- A mirror is composed of 38 spherical mirrors of 60 cm in diameter
- The mirror's radius of curvature is  
 $R = 8.5 \text{ m}$
- The angles of the mirror's turn  
azimuthal -  $0^\circ - 360^\circ$ ;  
zenith -  $0^\circ - 110^\circ$

- Accuracy of guidance of the telescope central axis  $< 0.1^\circ$
- Distance between the mirrors and the lightreceiver

$$F = 0.47 \quad R = 4.1 \text{ m}$$

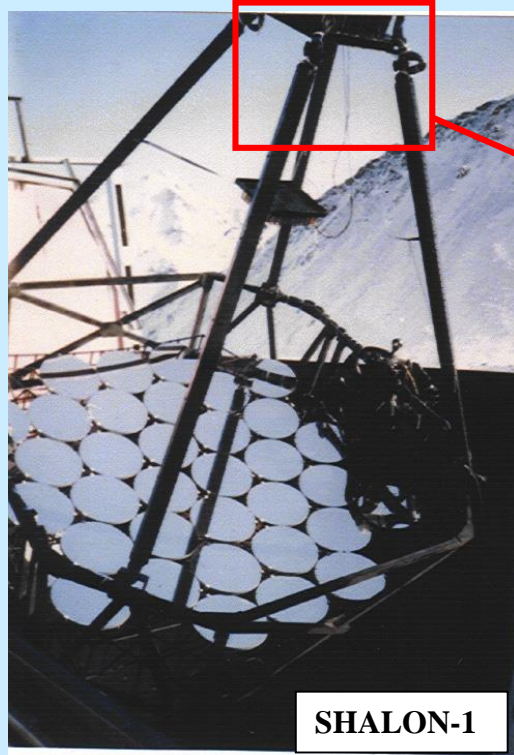
- Field of view  $> 8^\circ$
- Altazimuth mounting
- Parallactic mounting
- The mirror's weight -  $\sim 1 \text{ ton}$
- The weight of the lightreceiver 200 kg
- Total weight - 6 ton





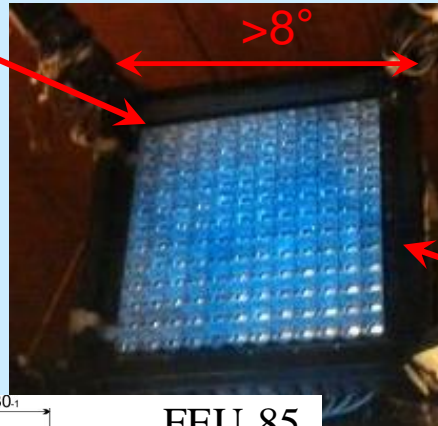
# SHALON OBSERVATORY

for 800 GeV – 100 TeV gamma-astronomy

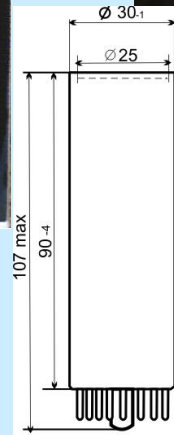


SHALON-1

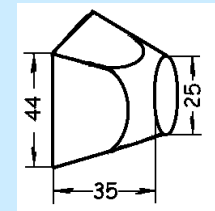
Sinitsyna, Int. Workshop VHE  
Gamma Ray Astronomy  
Crimia, (1989)



The idea of enhancement of angular resolution and sensitivity to the  $\gamma$ -rays with construction of the wide field of view was realized in SHALON telescopes since the construction in 1992



FEU-85



Metal square-cone lightguide is used to improve light collection



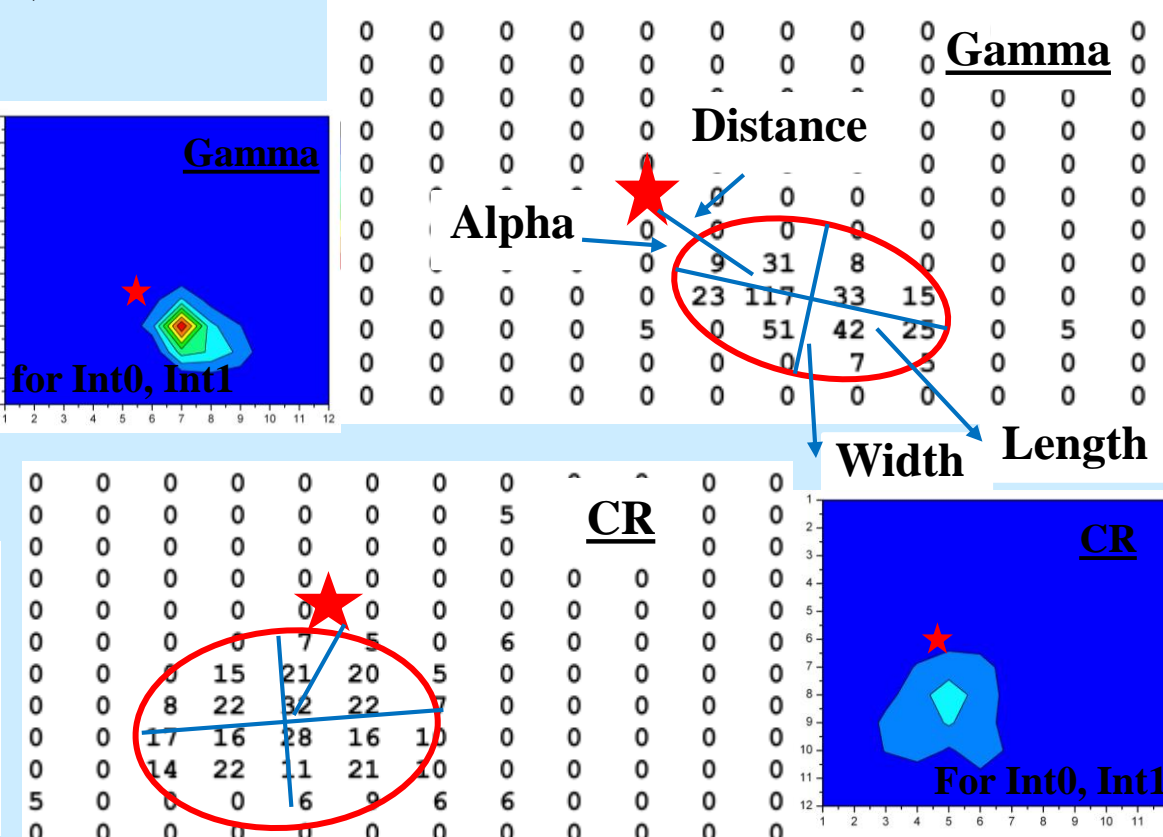
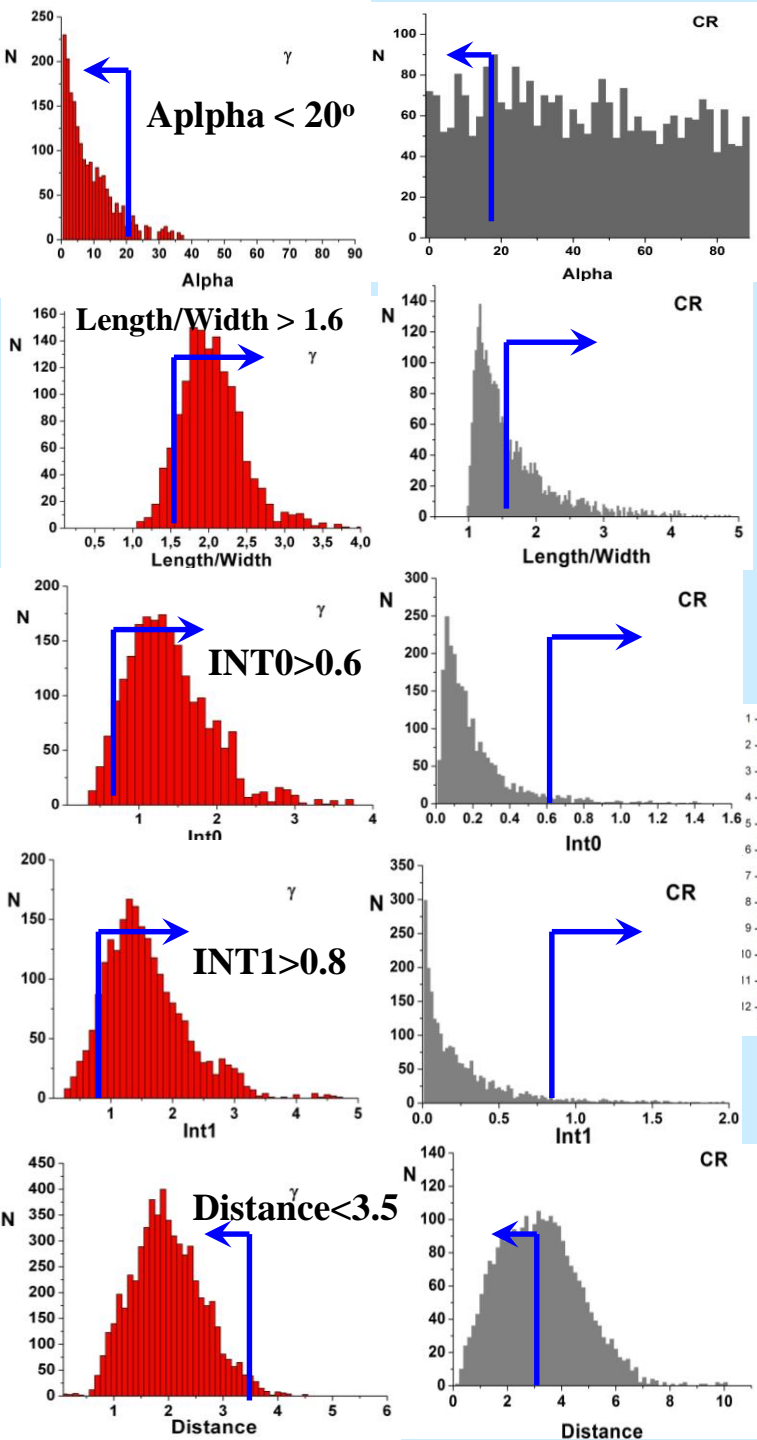
SHALON-2

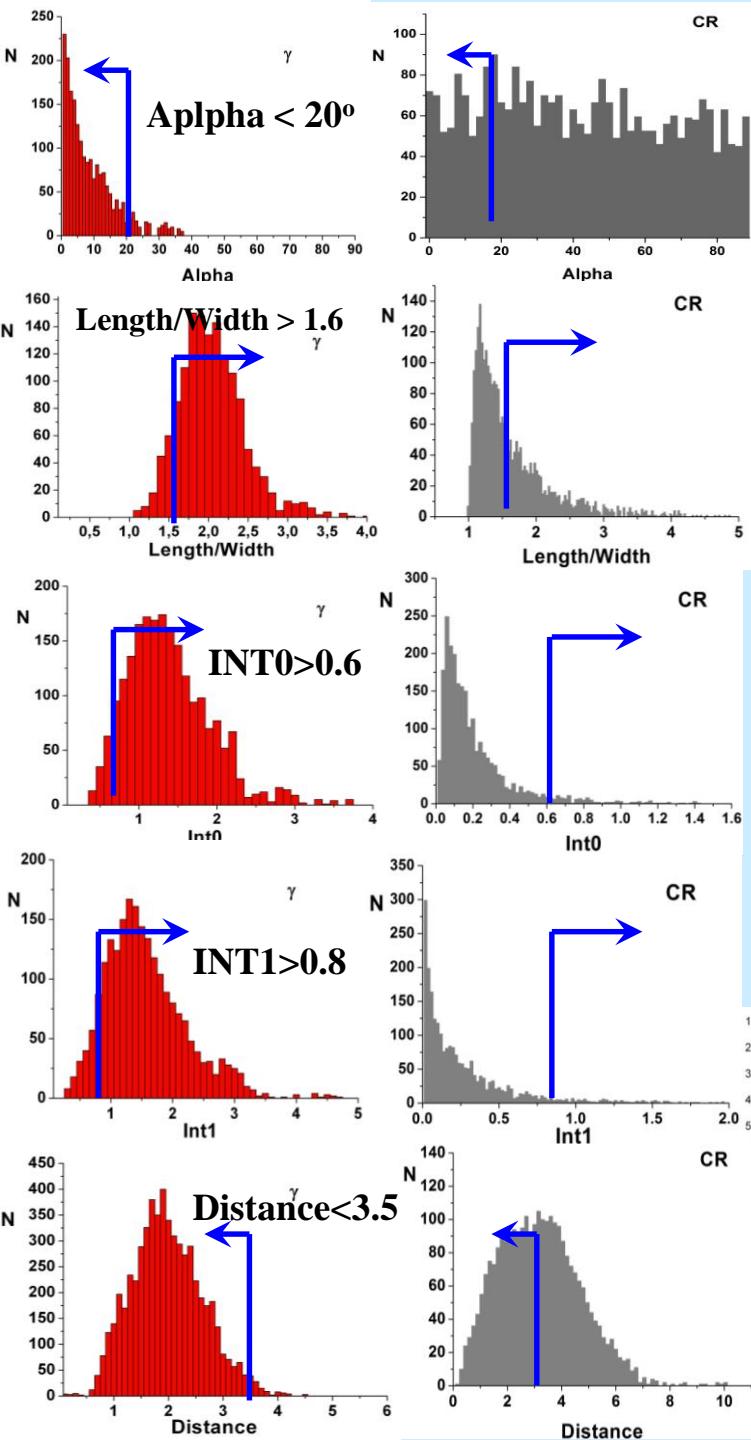
- The distance between the mirror and the lightreceiver  
 $F=0,47R=4.1m$
- Number of photomultipliers 144(12x12)
- Type of photomultipliers FEU-85 (PMT-85)
- The telescope's field of view  $>8^\circ$

## Criteria

The selection of gamma-initiated showers from the background of CR showers is performed by applying the following criteria:

- 1) **Alpha < 20°; 72% rejection**
- 2) **Length/Width > 1.6; 49% rejection**
- 3) the ratio **INT0** of Cherenkov light intensity in pixel with maximum pulse amplitude to the light intensity in the eight surrounding pixels exceeds **> 0.6; 92% rejection**
- 4) the ratio **INT1** of Cherenkov light intensity in pixel with maximum pulse amplitude to the light intensity in the in all the pixels except for the nine in the center of the matrix is exceeds **> 0.8; 88% rejection**
- 5) **Distance** is less than **3.5** pixels. **50% rejection**



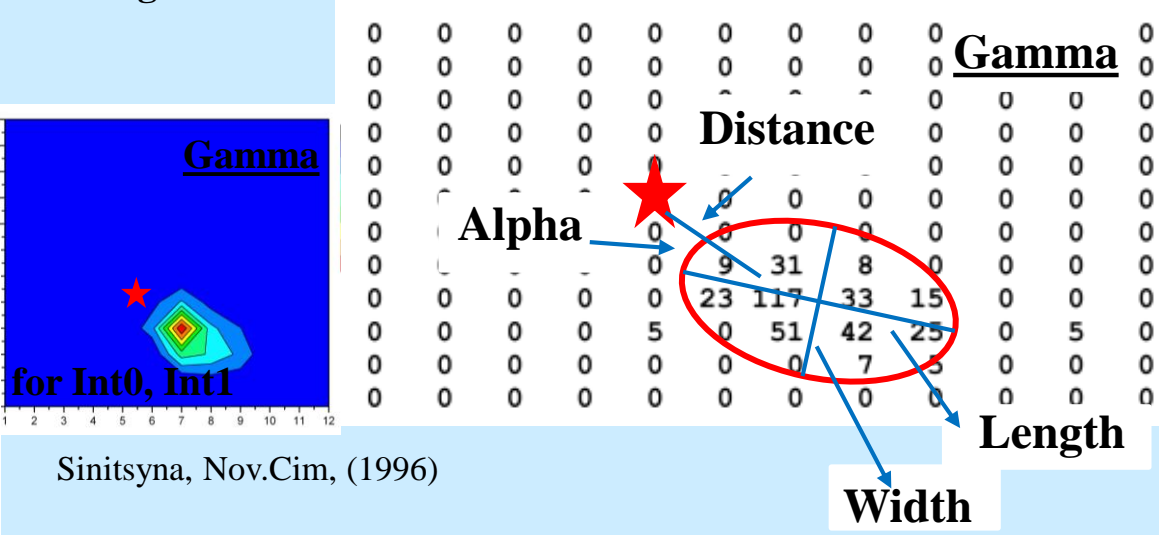


The selection of gamma-initiated showers from the background of CR showers is performed by applying the following criteria:

- 1) Alpha < 20°; 72% rejection
- 2) Length/Width > 1.6; 49% rejection
- 3) the ratio INT0 of Cherenkov light intensity in pixel with maximum pulse amplitude to the light intensity in the eight surrounding pixels exceeds > 0.6; 92% rejection
- 4) the ratio INT1 of Cherenkov light intensity in pixel with maximum pulse amplitude to the light intensity in the in all the pixels except for the nine in the center of the matrix is exceeds > 0.8; 88% rejection
- 5) Distance is less than 3.5 pixels. 50% rejection

It is essential that our telescope has a large matrix with full angle > 8° that allows us to perform observations of the supposed astronomical source (ON data) and background from extensive air showers (EAS) induced by cosmic ray (OFF data) simultaneously.

Using these criteria the background is rejected with 99.93% efficiency, whereas gamma's rejection is no more than 35% (that is taking into account).





# SHALON OBSERVATORY

## for 800 GeV – 100 TeV gamma-astronomy

The performance of Cherenkov telescope together with selection criteria is summarized by its angular resolution and gamma-ray flux sensitivity.

The accuracy of the determination of the coordinates of the  $\gamma$ -ray shower source in SHALON is  $\sim 0.07^\circ$  (Sinitsyna 2014) and it is increased by a factor of  $\sim 10$  after additional processing (Sinitsyna Astr.Lett 2014, 2018).

The sensitivity of the telescope is defined as the flux for 50 h of observation of a point-like source at a confidence level of  $5\sigma$  (according to the formulation of Li&Ma).

The SHALON minimum detectable integral flux of  $\gamma$ -rays at energy of 1 TeV is  $2.1 \times 10^{-13} \text{ cm}^{-2} \text{ s}^{-1}$ . In the region 1–50 TeV the minimum detectable flux falls down to the value of  $6 \times 10^{-14} \text{ cm}^{-2} \text{ s}^{-1}$  and then, at energies  $E > 50 \text{ TeV}$ , it grows because of limited telescopic field of view (Sinitsyna et al. Adv.Sp.R 2017, Sinitsyna Astr.Lett, 2018).

A photograph of the SHALON-1 Cherenkov telescope. It features a large, circular array of white, cylindrical photomultiplier tubes (PMTs) arranged in a hexagonal pattern. The array is mounted on a complex metal frame with several support legs. The background shows a snowy, mountainous landscape under a clear sky.

SHALON-1

A log-log plot showing the sensitivity of various gamma-ray telescopes. The y-axis is labeled  $F(>E), \text{ cm}^{-2} \text{ s}^{-1}$  and ranges from  $10^{-14}$  to  $10^{-10}$ . The x-axis is labeled  $E, \text{ TeV}$  and ranges from 0.01 to 100. The plot includes several curves: MAGIC-I (green dashed), MAGIC-II (magenta dashed), VERITAS (blue solid), CAT (black square), Whipple (black solid), MILAGRO, 5yr (blue dashed), HEGRA (green solid), HESS (red solid), and SHALON (red solid). The SHALON curve shows the lowest sensitivity (highest flux) in the 1-50 TeV range.

A photograph of the SHALON-2 Cherenkov telescope. It is similar to SHALON-1, with a large array of white PMTs mounted on a metal frame. The background is a clear blue sky.

SHALON-2

Sensitivity of  $\gamma$ -ray telescopes and detectors at 100 GeV – 100 TeV.

# SHALON OBSERVATORY

for 800 GeV – 100 TeV

gamma-astronomy

Operated since 1992

- Plerions
- Shell-type SNRs
- Flaring stars
- Binaries
- Seyfert Galaxies
- Radio Galaxies
- Blazars
- Flat spectrum radio-quazars



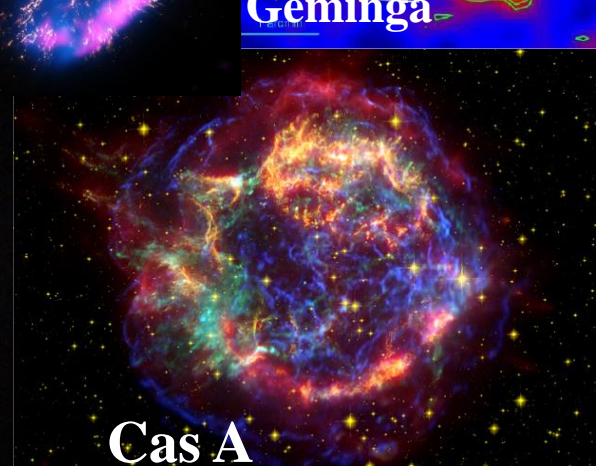
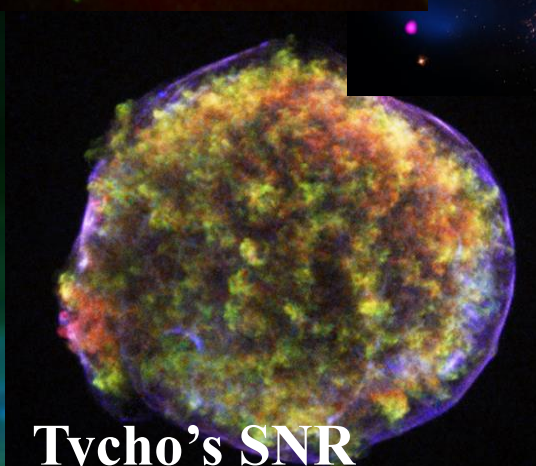
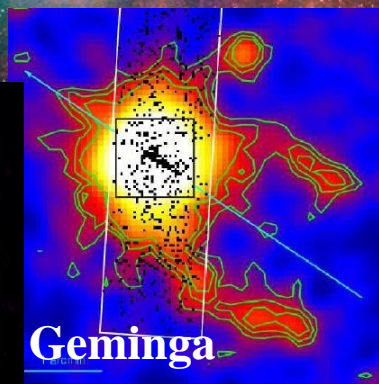
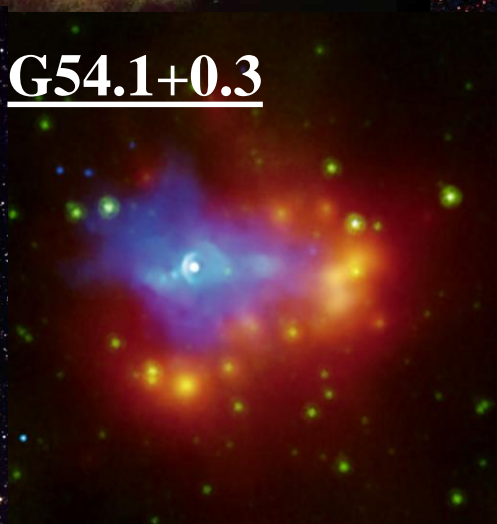
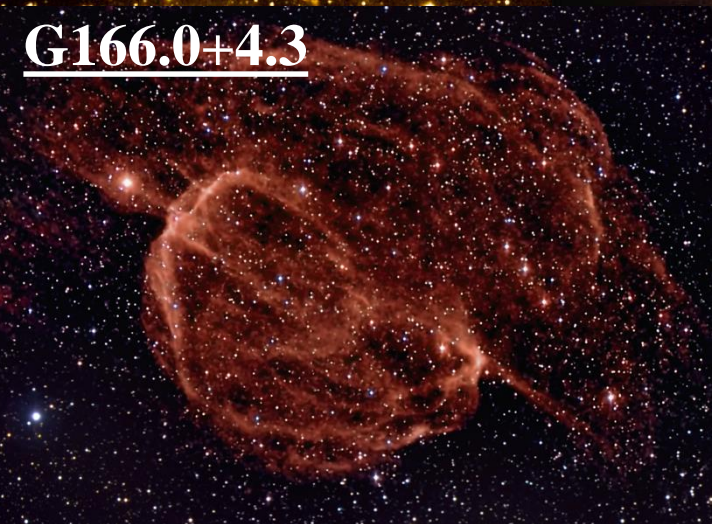
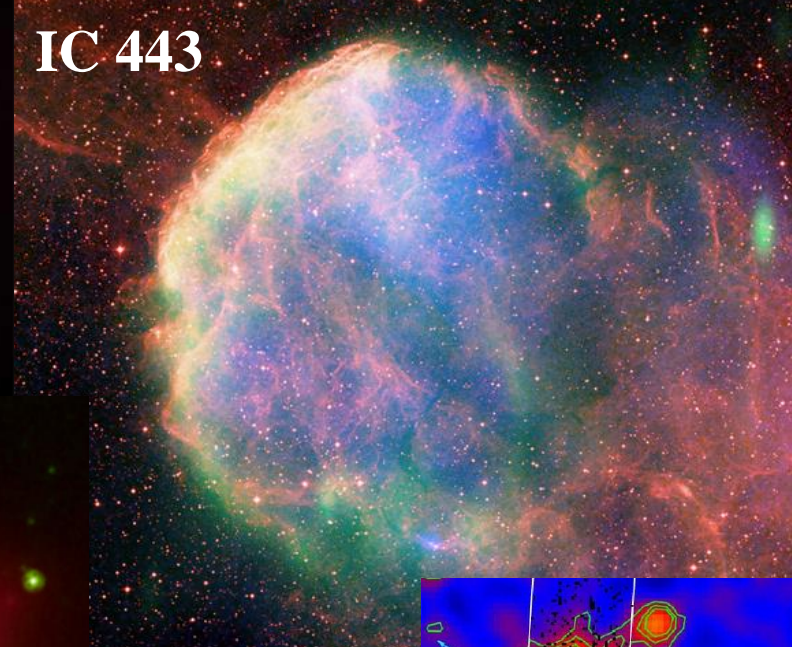
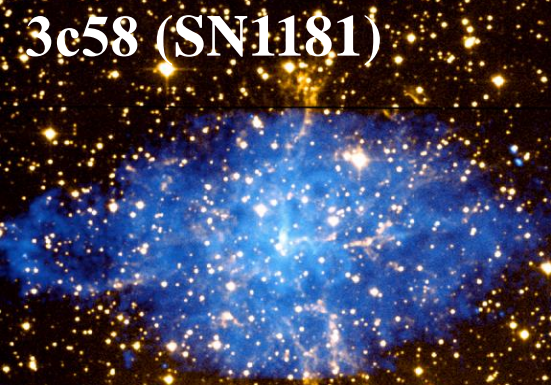


# SHALON catalogue of $\gamma$ -ray sources 800 GeV – 100 TeV (2018)

Source	Source type	Observed Flux, $\text{cm}^{-2}\text{s}^{-1}$	Distance		Detected** by SHALON	Detected at high energies Experiment/year	Detected at very high energies Experiment/year
<b><i>Galactic</i></b>			<i>kpc</i>				
Crab Nebula	Plerion, PWN	$(2.12 \pm 0.12) \times 10^{-12}$	2.0		1995 <sup>1</sup>	COS-B/1987 <sup>15</sup> (FermiLAT/2009)	Whipple/1989 <sup>16</sup>
* <b>Geminga</b>	Radio-weak pulsar/Plerion	$(0.48 \pm 0.07) \times 10^{-12}$	0.25		2000 <sup>5</sup>	COS-B/1981 <sup>18</sup> EGRET/1994 <sup>19</sup>	Crimea/2001 <sup>49</sup> MILAGRO/2007 <sup>20</sup>
* <b>3c 58</b>	Plerion, PWN	$(0.56 \pm 0.15) \times 10^{-12}$	2.6 - 3.2		2012 <sup>14</sup>	FermiLAT/2009 <sup>27</sup>	(VERITAS/2006 UL)
SNR 1181 (?)	Plerion, PWN (?)	$(1.40 \pm 0.43) \times 10^{-12}$	2.6 - 3.2 (?)		2012 <sup>14</sup>	FermiLAT/2009 <sup>27</sup>	—
G54.1+0.3	Plerion, PWN	$(0.97 \pm 0.35) \times 10^{-12}$	6.2		2015 ●	FermiLAT/2009	VERITAS/2010
* <b>GK Per(Nova1901)</b>	Classical Nova	$(0.31 \pm 0.14) \times 10^{-12}$	0.46		2015 <sup>54</sup> ●	—	—
* <b>Tycho's SNR</b>	Shell-type SNR	$(0.52 \pm 0.04) \times 10^{-12}$	2.5 – 3,5		1998 <sup>4</sup>	FermiLAT/2011 <sup>24</sup>	VERITAS/2011 <sup>23</sup>
Cas A	Shell-type SNR	$(0.64 \pm 0.10) \times 10^{-12}$	3,1		2011 <sup>12</sup>	FermiLAT/2010 <sup>26</sup>	HEGRA/2001 <sup>25</sup>
* <b>G166.0+4.3</b>	Shell-type SNR	$(1.07 \pm 0.46) \times 10^{-12}$	4.5		2016 ●		
IC 443	Shell-type SNR	$(1.69 \pm 0.58) \times 10^{-12}$	1.5		2012 <sup>14</sup>	EGRET/1996 <sup>21</sup> (FermiLAT/2009)	MAGIC/2007 <sup>22</sup>
* <b><math>\gamma</math>Cygni SNR</b>	Shell-type SNR	$(1.27 \pm 0.11) \times 10^{-12}$	1.5		2013 <sup>50</sup> ●	EGRET/1996 <sup>21</sup> (FermiLAT/2009)	VERITAS/2013 <sup>51</sup>
* <b>Cygnus X-3</b>	Binary	$(0.68 \pm 0.04) \times 10^{-12}$	10		1997 <sup>2</sup>	EGRET/1997 <sup>29</sup> (FermiLAT/2009 <sup>30</sup> )	Crimea/2009 <sup>48</sup> (Crimea/1975 <sup>28</sup> )
TeV J2032+4130	SNR or unresolved	$(0.84 \pm 0.05) \times 10^{-12}$	1.8?		2017 <sup>56</sup> ●		HEGRA/2002
* <b>2129+47XR</b>	Low-mass X-ray Binary	$(0.19 \pm 0.06) \times 10^{-12}$	6.0		2006 <sup>7</sup>	—	—
* <b>Her X-1</b>	Binary	$(0.45 \pm 0.18) \times 10^{-12}$	6.6		2012	—	(Whipple UL)
* <b>M57</b>	Planetary nebula	$(0.30 \pm 0.17) \times 10^{-12}$	0.7		2011 <sup>13</sup>	—	—
* <b>V1589 Cyg</b>	Red dwarf	$(0.12 \pm 0.02) \times 10^{-12}$	0.023-0.032		2018 ●		
* <b>V962 Tau</b>	Red dwarf	$(0.38 \pm 0.07) \times 10^{-12}$	?		2018 ●		
* <b>V780 Tau</b>	Red dwarf	$(0.21 \pm 0.04) \times 10^{-12}$	0.01		2018 ●		
* <b>V388 Cas</b>	Red dwarf	$(1.10 \pm 0.21) \times 10^{-12}$	0.009-0.01		2018 ●		
<b><i>Extragalactic</i></b>			<i>Mpc</i>	<i>z</i>			
* <b>NGC 1275</b>	Seyfert Galaxy	$(0.78 \pm 0.05) \times 10^{-12}$	71	0.0179	1997 <sup>3</sup>	FermiLAT/2009 <sup>31</sup>	MAGIC/2012 <sup>32</sup>
* <b>SN2006 gy</b>	Extragal. Supernova	$(3.71 \pm 0.65) \times 10^{-12}$	73	0.019	2007 <sup>9</sup>	—	—
IC 310	Radio Galaxy	$(0.89 \pm 0.09) \times 10^{-12}$	81	0.019	2017 ●	FermiLAT/2010	MAGIC/2010
Mkn 421	BLLac	$(0.63 \pm 0.05) \times 10^{-12}$	124	0.031	1995 <sup>1</sup>	EGRET/1992 <sup>35</sup> (FermiLAT/2009)	Whipple/1992 <sup>33</sup>
Mkn 501	BLLac	$(0.86 \pm 0.06) \times 10^{-12}$	135	0.034	1997 <sup>1a</sup>	EGRET/1999 <sup>37</sup> (FermiLAT/2009)	Whipple/1996 <sup>34</sup>
Mkn 180	BLLac	$(0.65 \pm 0.09) \times 10^{-12}$	173	0.046	2009 <sup>10</sup>	FermiLAT/2009 <sup>39</sup>	MAGIC/2006 <sup>38</sup>
* <b>3C382</b>	Broad Line Radio Galaxy	$(0.95 \pm 0.33) \times 10^{-12}$	230	0.058	2010 <sup>11</sup>	(FermiLAT UL) <sup>40</sup>	—
* <b>4C+31.63</b>	FSRQ	$(0.72 \pm 0.22) \times 10^{-12}$	1509	0.295	2013 ●	FermiLAT/2010 <sup>47</sup>	—
* <b>OJ 287</b>	BLLac	$(0.26 \pm 0.07) \times 10^{-12}$	1576	0.306	2005 <sup>8</sup> (UL) 2010 <sup>11</sup>	FermiLAT/2009 <sup>41</sup>	(MAGIC / 2009 UL) <sup>42</sup>
* <b>3C454.3</b>	FSRQ	$(0.43 \pm 0.07) \times 10^{-12}$	5489	0.859	2000 <sup>6</sup>	FermiLAT/2009 <sup>44</sup>	(MAGIC / 2009 UL) <sup>45</sup>
* <b>4C+55.17</b>	FSRQ	$(0.91 \pm 0.25) \times 10^{-12}$	5785	0.896	2013 ●	FermiLAT/2011 <sup>43</sup>	—
PKS 1441+25	FSRQ	$(0.52 \pm 0.23) \times 10^{-12}$	6133	0.939	2016 ●	FermiLAT/2015	VERITAS/2015 <sup>55</sup>
* <b>1739+522 (4c+51.37)</b>	FSRQ	$(0.49 \pm 0.05) \times 10^{-12}$	9913	1.375	2000 <sup>6</sup>	FermiLAT/2010 <sup>46</sup>	—
* <b>B2 0242+43</b>	FSRQ	$(0.58 \pm 0.20) \times 10^{-12}$	16865	2.243	2015 ●	FermiLAT/2010, 2011	—
* <b>B2 0743+25</b>	FSRQ	$(0.37 \pm 0.16) \times 10^{-12}$	23466	2.949	2015 ●	FermiLAT/2010, 2011	—

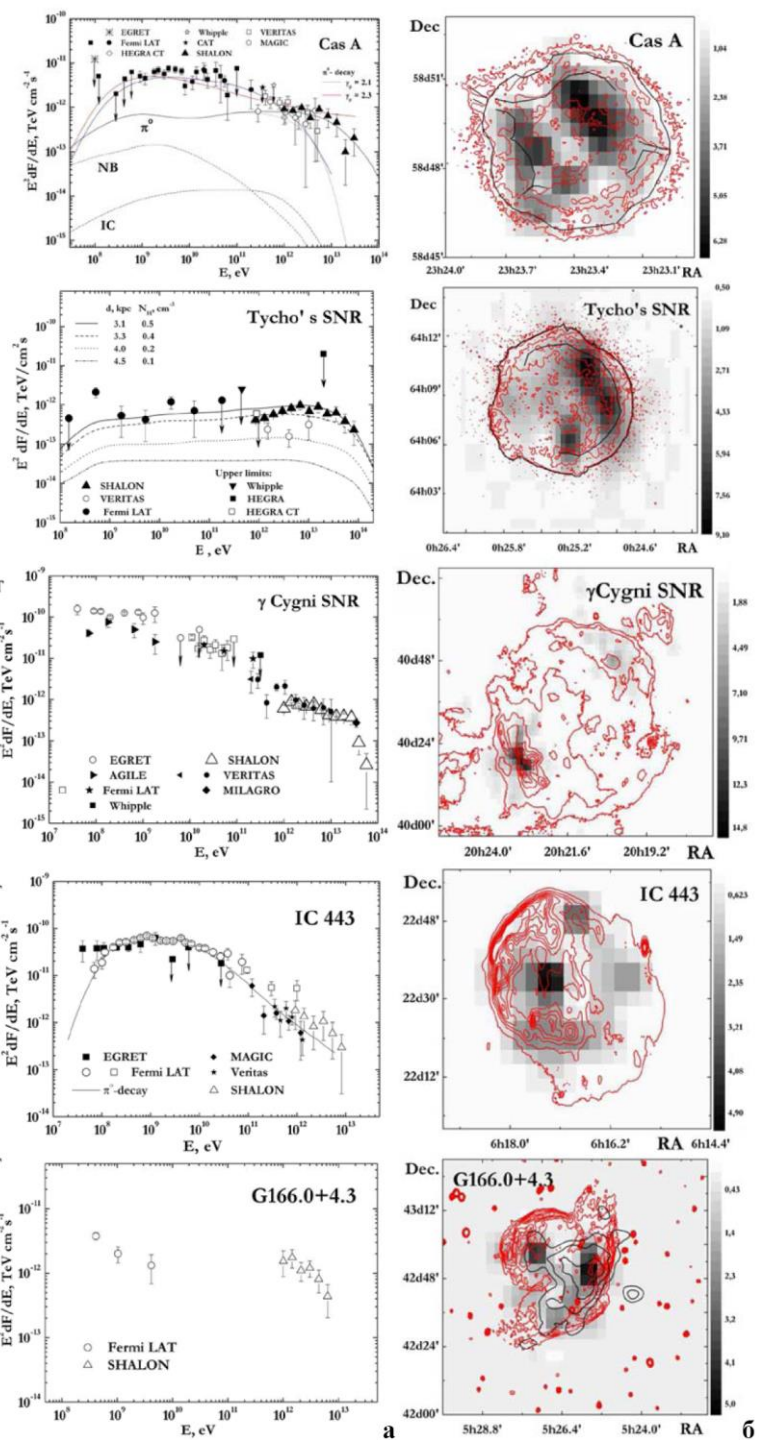


# TeV Gamma-ray emission from Supernova Remnants





# Shell-type Supernova Remnants



Supernova Remnants (SNRs) have long been considered as unique candidates for cosmic-ray sources. Direct data on the distribution of cosmic rays in SNRs can be obtained from very high energy gamma-ray observations. As the presence of the electron cosmic-ray component is clearly seen by the emission generated by it in an SNR in a wide wavelength range, from radio to high-energy gamma-rays, while the nuclear cosmic-ray component can be detected only by very high energy  $\gamma$ -ray emission. The SHALON observations have yielded the results on Galactic supernova remnants (SNR) of different ages. Among them are: the shell-type SNRs Tycho's SNR (1572 y), Cas A (1680 y), IC 443 (age 300 - 30000 y),  $\gamma$ Cygni SNR (age 5000 - 7000 y), G166.0+4.3 (age 24000 y). For each of SNRs the observation results are presented with spectral energy distribution by SHALON in comparison with other experiment data and images by SHALON in together with data from X-ray by Chandra and radio-data by CGPS. For the first time it was shown the location of TeV gamma-ray emission regions relative to the position SNR's remarkable features as a forward and reverse shocks, dense molecular clouds swept out by SNR explosion and shells due to the interaction of the supernova ejecta and the surrounding medium. The collected experimental data have confirmed the prediction of the theory about the hadronic generation mechanism of very high energy 800 GeV–100 TeV gamma-rays in Tycho's SNR, Cas A, IC 443 and  $\gamma$ Cygni SNR.

1. V.G. Sinitsyna, V.Y. Sinitsyna, S.S. Borisov, I.A. Ivanov, A.I. Klimov, R.M. Mirzafatikhov, N.I. Moseiko, 2017, *Advances in Space Research*, doi:10.1016/j.asr.2017.04.007.
2. V.G. Sinitsyna, M.S. Andreeva, K.A. Balygin, S.S. Borisov, I.A. Ivanov, A.M. Kirichenko, A.I. Klimov, I.P. Kozhukhova, R.M. Mirzafatikhov, N.I. Moseiko, I.E. Ostashev, V.Y. Sinitsyna, I.G. Volokh, 2017, *EPJ Web of Conferences*, v. 145, 19003. doi:1051/epjconf/201614519003.

**Table 1.** The catalogue of galactic  $\gamma$ -ray sources by SHALON with parameters for spectrum fitting in form of power law with exponential cutoff  $F(> E) \propto E^{k_\gamma} \times \exp(-E/E_{\text{cutoff}})$ .

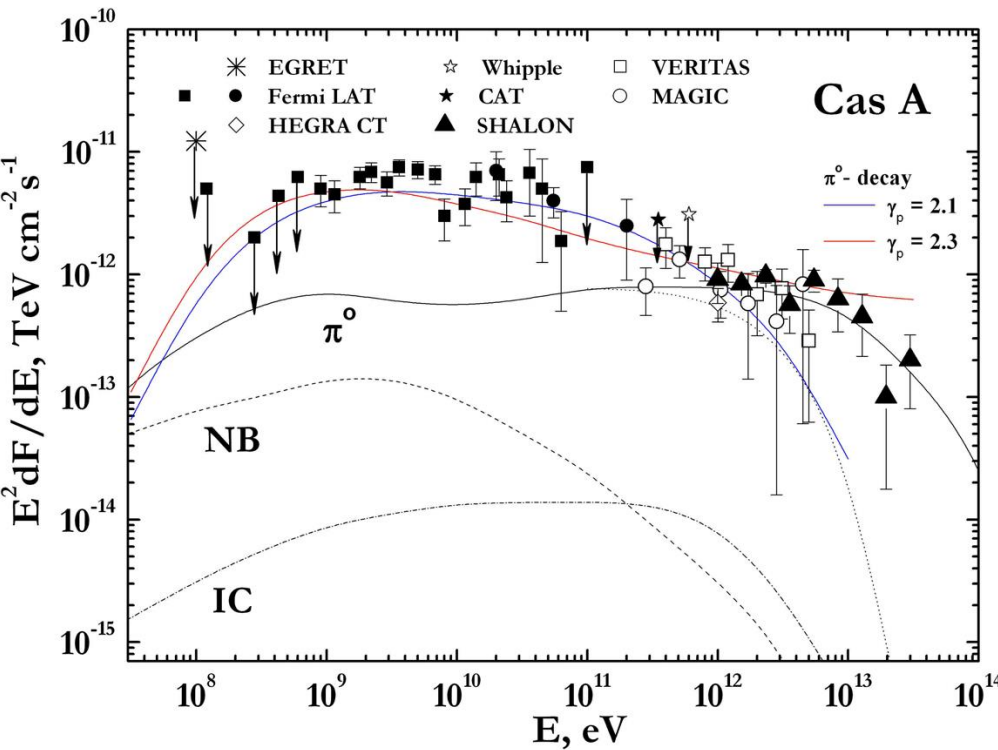
Sources	Observable flux <sup>a</sup>	$k_\gamma$	$E_{\text{cutoff}}$ , TeV	Distance, kpc	Type
Crab Nebula	$(2.12 \pm 0.12)$	$-1.36 \pm 0.09$	$19.0 \pm 2.0$	2.0	PWN
Geminga	$(0.48 \pm 0.07)$	$-0.39 \pm 0.05$	$5.4 \pm 1.0$	0.25	PSR or PWN
3C 58	$(0.56 \pm 0.15)$	$-1.33 \pm 0.12$	—	3.2	PWN
G54.1+0.3	$(0.97 \pm 0.35)$	$-1.43 \pm 0.14$	—	6.2	PWN
Tycho's SNR	$(0.52 \pm 0.04)$	$-0.93 \pm 0.09$	$35.0 \pm 5.0$	3.1–3.3	Shell-type SNR
Cas A	$(0.64 \pm 0.10)$	$-0.91 \pm 0.11$	$10.3 \pm 2.5$	3.1	Shell-type SNR
IC 443	$(1.69 \pm 0.58)$	$-1.94 \pm 0.16$	—	1.5	Shell-type SNR
G166.0+4.3	$(1.07 \pm 0.46)$	$-1.95 \pm 0.44$	—	4.5	Shell-type SNR
$\gamma$ Cygni SNR	$(1.27 \pm 0.11)$	$-0.93 \pm 0.09$	$20.1 \pm 4.2$	1.5	Shell-type SNR
GK Per	$(0.31 \pm 0.14)$	$-1.90 \pm 0.36$	—	0.46	Classical Nova
Cyg X-3	$(0.68 \pm 0.04)$	$-1.15 \pm 0.08$	$75.0 \pm 10.2$	10.0	HMX Binary
4U 2129+47	$(0.19 \pm 0.06)$	$-0.42 \pm 0.12$	$10.0 \pm 3.0$	6.0	LMX Binary
Her X-1	$(0.45 \pm 0.18)$	—	—	6.6	LMX Binary
M57	$(0.30 \pm 0.17)$	—	—	0.7	Planetary nebula

<sup>a</sup>Integral flux at energy  $> 800$  GeV in units of  $10^{-12} \text{ cm}^{-2} \text{ s}^{-1}$





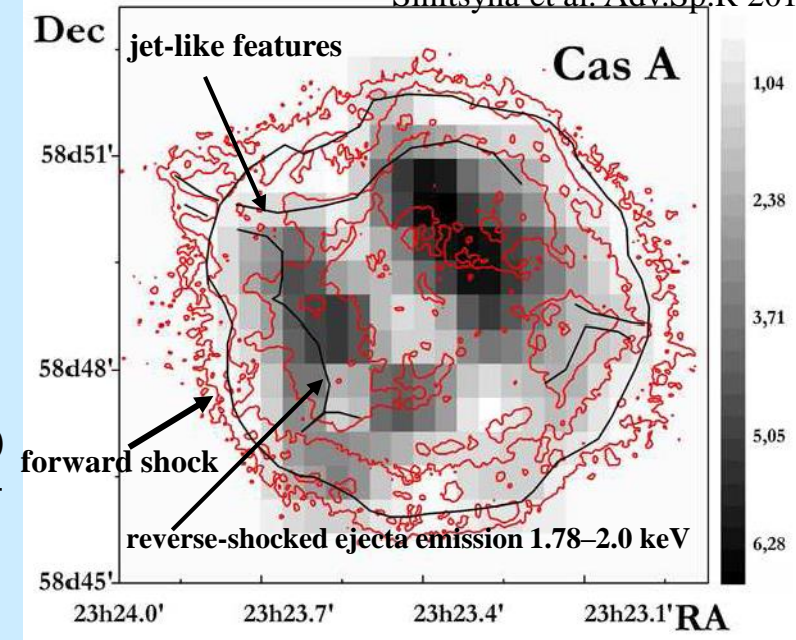
# Cassiopeia A (1680 yr.)



The favored scenarios in which the  $\gamma$ -rays of 500 MeV – 10 TeV energies are emitted in the shell of the SNR like Cas A are Inverse Compton scattering and  $\pi^0$ -decay. The  $\gamma$ -ray emission could be produced by electrons accelerated at the forward shock through relativistic bremsstrahlung (NB) or IC. Alternatively, the GeV  $\gamma$ -ray emission could be produced by accelerated CR hadrons through interaction with the background gas and then  $\pi^0$ -decay.

Solid lines show the very high energy  $\gamma$ -ray spectra of hadronic origin. Dash-and-dot line presents the *gamma*-ray spectrum of the IC emission. It was shown that leptonic model with  $B = 0.3$  mG predicts a 5 - 8 times lower  $\gamma$ -ray flux than the observed; the model with  $B = 0.12$  mG, which can broadly explain the observed GeV flux predicts the TeV spectrum with cut-off energy about 10 TeV.

Sinitsyna et al. Adv.Sp.R 2017



The spectral energy distribution of the  $\gamma$ -ray emission from Cas A by SHALON ( $\blacktriangle$ ) in comparison with other experiment data Fermi LAT, HEGRA, MAGIC, VERITAS, EGRET, CAT, Whipple and with theoretical predictions [Abdo et al. 2010; Berezhko E G, Pühlhofer G, Völk H J, 2003] .

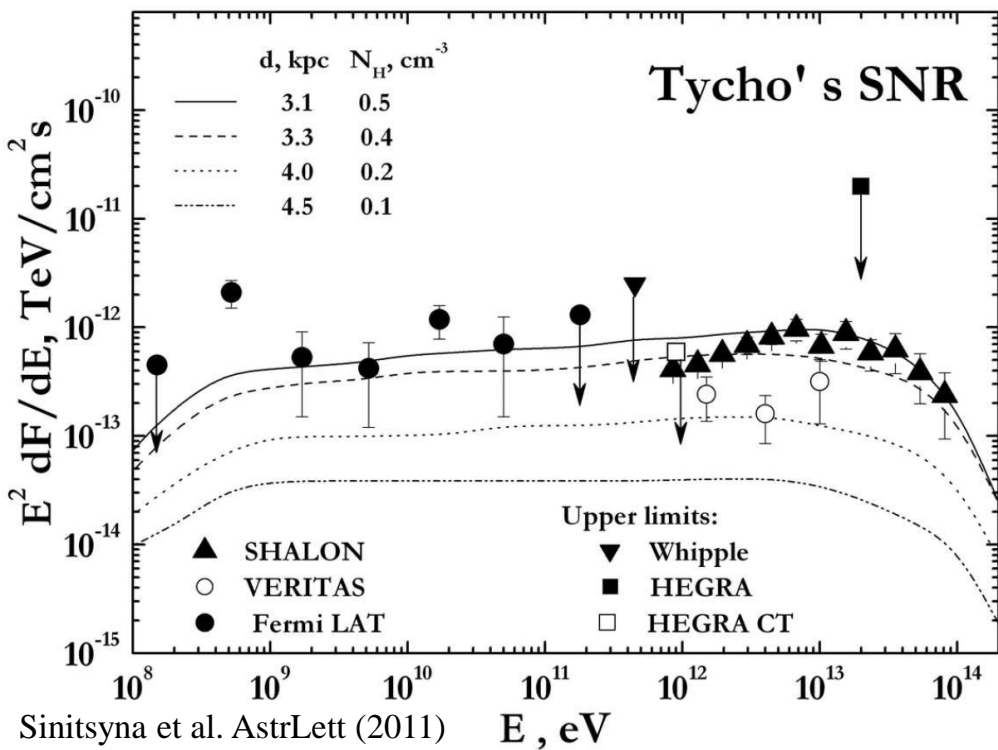
The  $\gamma$ -ray source associated with the Cas A SNR was detected above 800 GeV in observations of 2010 – 2014 yy. with a statistical significance of  $19.1\sigma$  Li&Ma with a  $\gamma$ -ray flux above 0.8 TeV :

$$I_{\text{CasA}}(>0.8\text{TeV}) = (0.64 \pm 0.10) \times 10^{-12} \text{ cm}^{-2}\text{s}^{-1}$$

The detection of very high energy  $\gamma$ -ray emission at 5 - 30 TeV and the hard spectrum below 1 TeV would favor the  $\pi^0$ -decay origin of the  $\gamma$ -rays in Cas A SNR

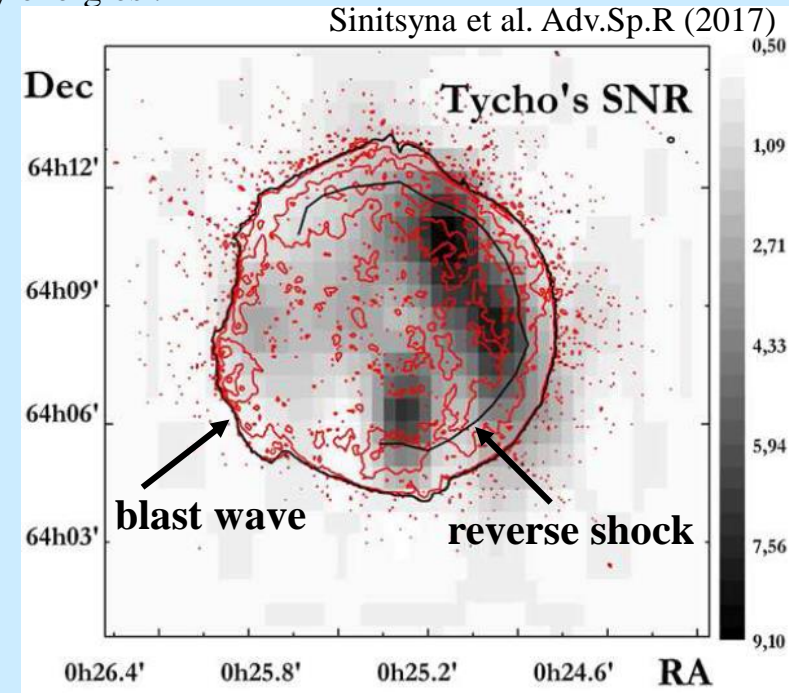
Chandra image of Cas A (X-ray) red lines ;  
The grey scale image shows the TeV-image by SHALON

# Tycho's SNR (1572yr)



The expected flux of  $\gamma$ -rays from  $\pi^0$ -decay, extends up to  $>30 \text{ TeV}$ , while the flux of  $\gamma$ -rays originated from the Inverse Compton scattering has a sharp cut-off above the few TeV, so the detection of  $\gamma$ -rays with energies up to  $80 \text{ TeV}$  by SHALON is an evidence of their hadronic origin. The additional information about parameters of Tycho's SNR can be predicted (in frame of nonlinear kinetic model with  $E_{\text{SN}} = 1.2 \times 10^{51} \text{ erg}$ ) if the TeV  $\gamma$ -ray spectrum of SHALON telescope is taken into account: a source distance  $3.1 - 3.3 \text{ kpc}$  and an ambient density  $N_H = 0.5 - 0.4 \text{ cm}^{-3}$  and the expected  $\pi^0$ -decay  $\gamma$ -ray energy extends up to about  $100 \text{ TeV}$ .

The same parameters have obtained in Kosenko et al. (2011) calculations of structures visible by Chandra at X-ray energies.



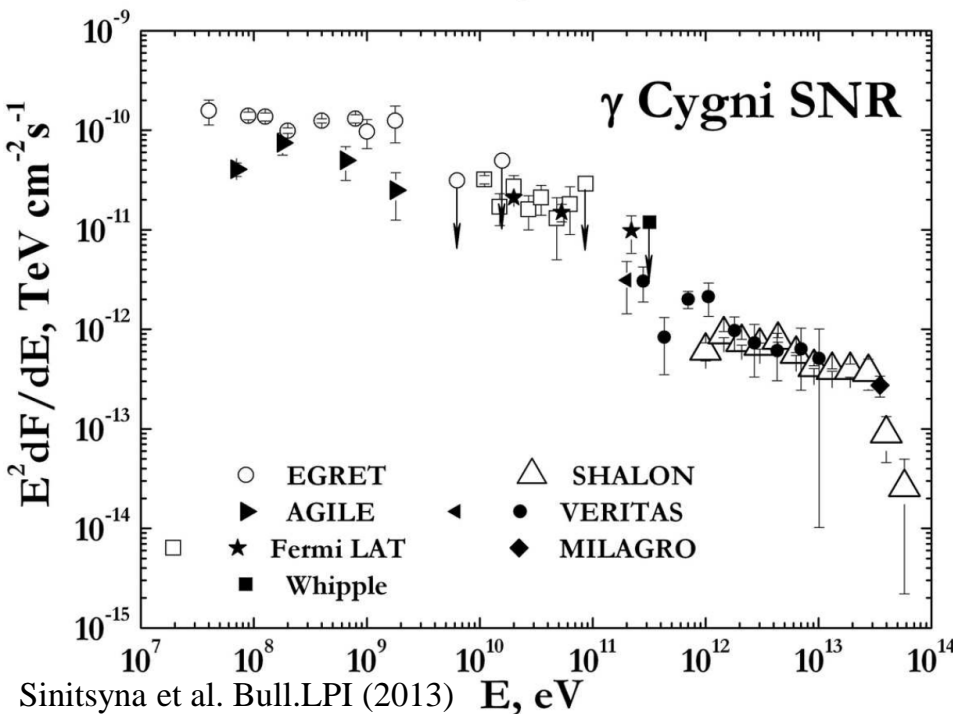
Recently, Tycho's SNR was also detected at GeV energy range by Fermi LAT (●) (2010, 2011). The Tycho's SNR spectral energy distribution by SHALON (▲) (1996 - 2010) comparing with VERITAS (○) (2009), Fermi LAT (●) (2010, 2011) and theoretical models [Volk H.J. Berezhko E.G. Ksenofontov L.T., 2008].

In observations of 1996 year a new galactic source was detected by SHALON5 in TeV energies. This object was identified with Tycho's SNRs with integral flux of  $(0.52 \pm 0.04) \times 10^{-12} \text{ cm}^{-2} \text{s}^{-1}$ . statistical significance of  $17\sigma$  Li&Ma.

**The image of Tycho's SNR by SHALON (grey scale);**  
**Red lines - Chandra X-ray image of Tycho's SNR**



# $\gamma$ Cygni SNR (age of $\sim (5 \div 7) \times 10^3$ years)

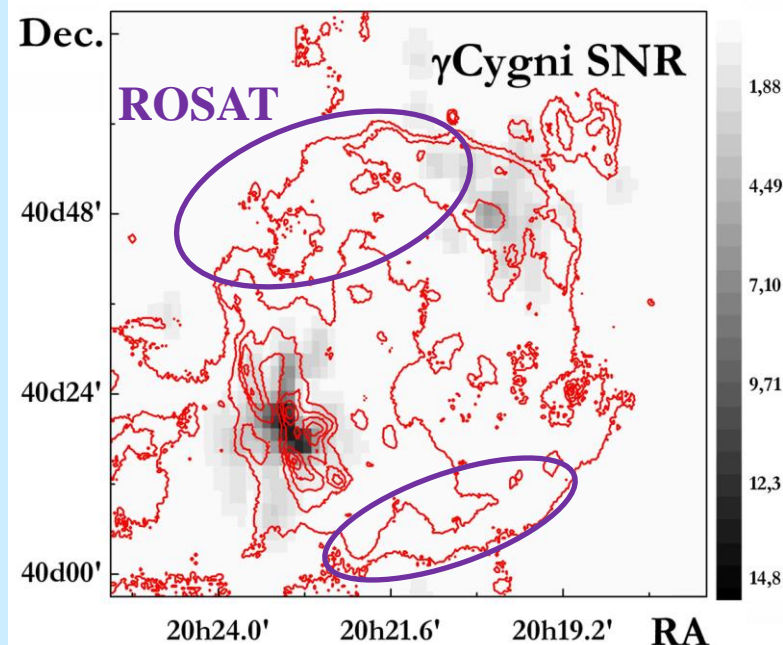


$\gamma$ Cygni SNR is a shell-type SNR at a distance of  $\sim 1 - 2$  kpc and with the observed diameter of  $\sim 1^\circ$ .  $\gamma$ Cygni SNR is older than Cas A and Tycho's SNR, its age is estimated as  $\sim 5000 - 7000$  yr. and its supposed to be in an early phase of adiabatic expansion.

$\gamma$ Cygni SNR as a source accompanying to Cyg X-3 is systematically studied with SHALON telescope since 1995y.  $\gamma$ Cygni SNR was observed with SHALON telescope during the period from 1995 till now for a total of 240 hours. The  $\gamma$ -ray source associated with the  $\gamma$ Cygni SNR was detected above 800 GeV with average  $\gamma$ -ray flux above 0.8 TeV:

$$I_{\gamma\text{Cygni SNR}}(>0,8\text{TeV}) = (1,27 \pm 0,11) \times 10^{-12} \text{ cm}^{-2}\text{s}^{-1}$$

The visible SNR features observed at X-rays, radio as well as TeV  $\gamma$ -ray emission can be result of the presents of shock at the interaction of the supernova ejecta and the surrounding medium.

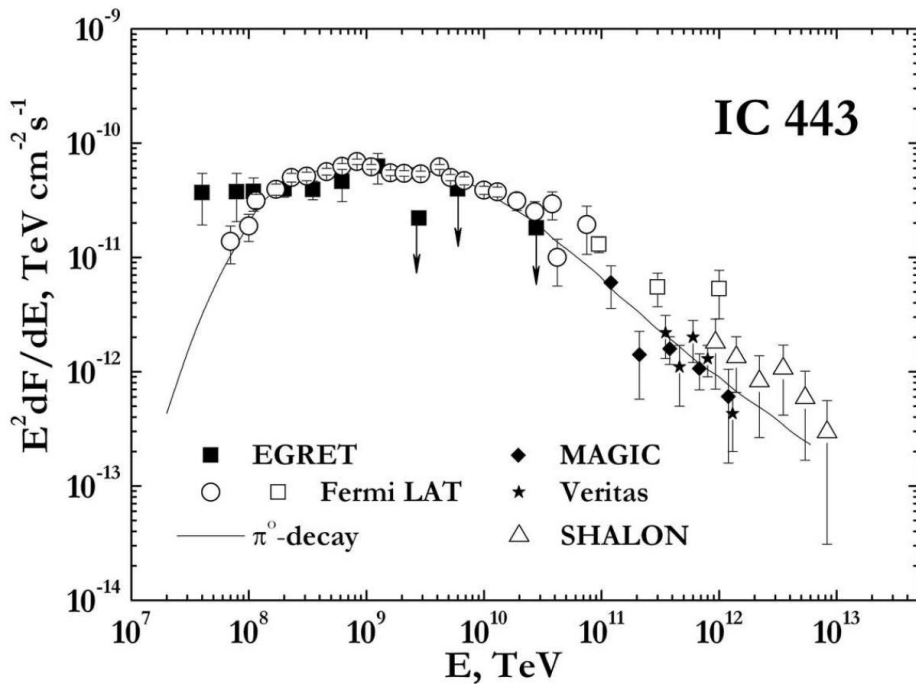


The spectral energy distribution of the  $\gamma$ -ray emission from  $\gamma$ Cygni SNR by SHALON ( $\Delta$ ) in comparison with other experiment data.

Very high energy  $\gamma$ -ray emission in shocks could be produced first via inverse-Compton scattering of accelerated electrons. Such high energy electrons should also produce X-ray synchrotron radiation visible in a non-thermal power-law in the X-ray spectrum. But no evidence for a non-thermal component of X-ray spectrum in North-West part of TeV shell and no source of the X-ray emission were detected at the location of SE TeV emission region. Also, the TeV  $\gamma$ -ray emission can originate from the shock acceleration of hadrons interacting with target material. The density of target material of SNR surroundings is enough to produce the observable TeV flux at the both regions via the shock acceleration of hadrons.

**Thus, the detection of  $\gamma$ -ray emission at 0.8–50 TeV by SHALON from the North-West and South-East regions of  $\gamma$ Cygni SNR would favor the  $\pi^0$ -decay origin of the  $\gamma$ -rays in this SNR.**

# IC 443 SNR (age of $\sim (3 \div 30) \times 10^3$ years)



The favored scenario in which the  $\gamma$ -rays of 100 MeV–10 TeV energies are emitted in the shell of the IC443 SNR is  $\pi^0$ -decay which produced in the interactions of the cosmic rays with the interstellar gas. Inverse Compton scattering can not explain the observed IC 443 gamma-ray emission as there is no bright source of seed photons in the region of the IC 443.

The analysis of SHALON observation results for IC 443 SNR in 800 GeV–10 TeV revealed the correlation of TeV  $\gamma$ -ray emission maxima with MeV-GeV emission observed by Fermi LAT and the overlapping of the location of swept out dense molecular cloud with the position of TeV  $\gamma$ -ray emission of South and South-West parts of IC 443 shell.

IC 443 was detected in TeV  $\gamma$ -rays, first by MAGIC (2007) and later confirmed by VERITAS (2009) and SHALON (2011) ( $\Delta$ ). The high energy  $\gamma$ -ray emission from IC 443 was detected with EGRET (1995) and then with Fermi LAT (2010) in the range 500 MeV - 50 GeV. Solid line shows the very high energy  $\gamma$ -ray spectra of hadronic origin.

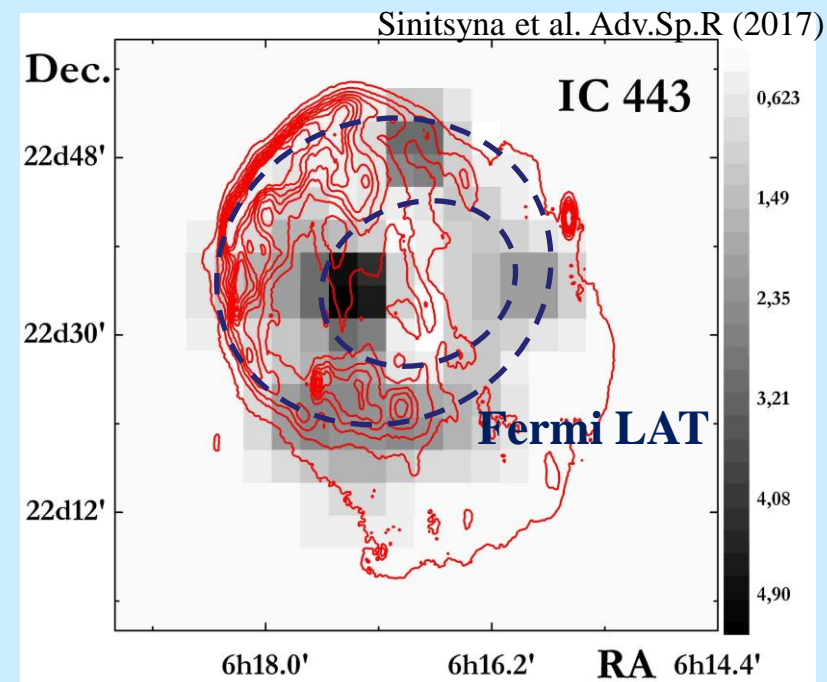
IC 443 was detected by SHALON with the integral flux above 0.8TeV:

$$I_{\text{IC 443}}(>0,8\text{TeV}) = (1,69 \pm 0,58) \cdot 10^{-12} \text{ cm}^{-2} \text{ s}^{-1}$$

with a statistical significance of  $9.7\sigma$  (Li&Ma).

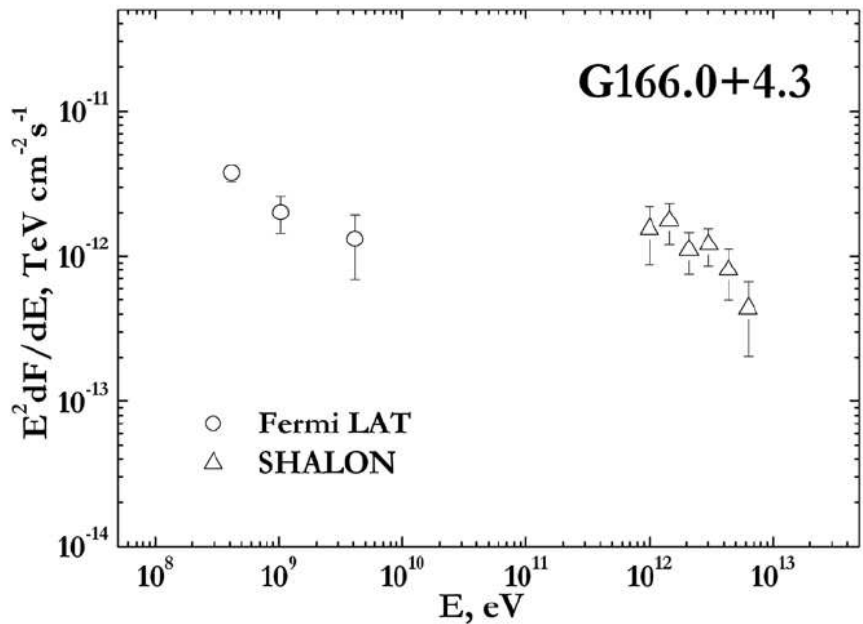
CGPS image of IC 443 (radio) red lines ;

The grey scale image shows the TeV-image by SHALON





# G166.0+4.3 SNR (age of $\sim 24 \times 10^3$ years)



Spectral energy distribution of very high energy  $\gamma$ -ray emission of G166.0+4.3 by SHALON (2016) (Sinitsyna et al. Adv.Sp.R 2017) and Fermi LAT.

G166.0+4.3 (VRO 42.05.01) is a supernova remnant with unusual morphology, contains a shell of circular component in northeast intersected by a larger bowl-shaped component in southwest (the wing), expanding into a low density medium. As such remnant morphology can be results from the shock encountering a density discontinuity in the interstellar medium, G166.0+4.3 became a candidate for the investigation of particle acceleration in SNR shocks at high- and very high energies. The TeV  $\gamma$ -ray emission regions correlate with the North-East and South-West parts of components visible in the radio energies by CGPS (red contours). But TeV emission is more significant near the West, where the extended wing component and maximum of X-ray emission viewed by ROSAT (black contours) are located.

**The grey scale image shows the TeV-image by SHALON**

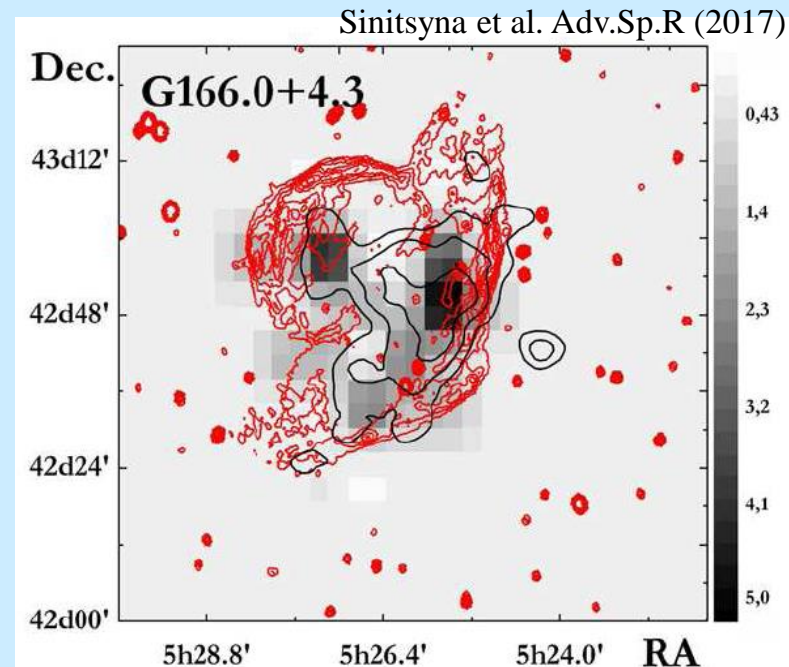
G166.0+4.3 was observed with SHALON telescope during the 20.1 h in period of 2015–2016 years. The gamma-ray source associated with the G166.0+4.3 SNR was detected above 800 GeV with a statistical significance of 6.1  $\sigma$  with a gamma-ray flux above 0.8 TeV of:

$$I_{G166+4.3}( > 0.8 \text{ TeV}) = (1.49 \pm 0.25) \cdot 10^{-12} \text{ cm}^{-2} \text{s}^{-1}$$

The energy spectrum of gamma-rays in the observed energy region from 0.8 TeV to 7 TeV is well described by the power law:

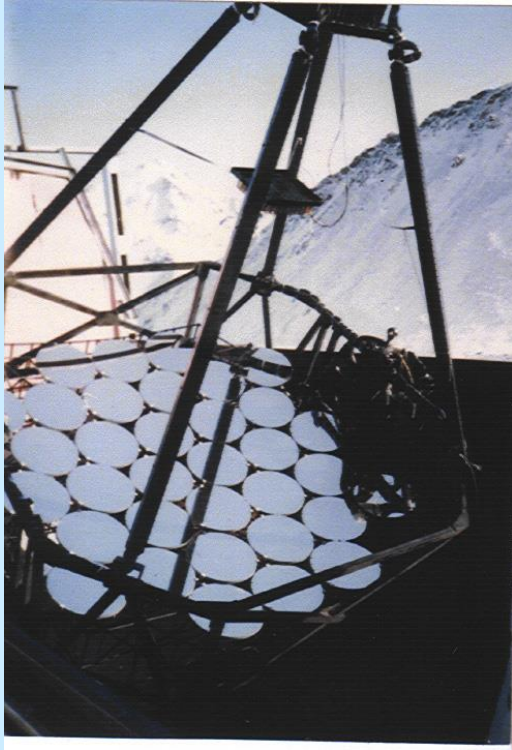
$$I(> E_\gamma) = (1.49 \pm 0.25) \times 10^{-12} \times E_\gamma^{-1.95 \pm 0.44}$$

For the first time very high energy  $\gamma$ -ray emission of circular and “wing” components of G166.0+4.3 was detected by SHALON.



Sinitsyna et al. Adv.Sp.R (2017)

# The very high energy characteristics of shell-type SNRs at different ages



The observation results of Galactic shell-types supernova remnants on different evolution stages **Cas A (1680 yr), Tycho's SNR (1572yr),  $\gamma$ Cygni SNR age of  $(5\div 7)\times 10^3$ yr, IC443 age of  $(3\div 30)\times 10^3$  yr and G166.0+4.3 age of  $24\times 10^3$  yr** by SHALON mirror Cherenkov telescope are presented. For the old supernova remnant G166.0+4.3 the very high energy  $\gamma$ -ray emission of circular and “wing” components of this SNR was detected by SHALON. For the first time it was shown the location of TeV gamma-ray emission regions relative to the position SNR's remarkable features as a forward and reverse shocks, dense molecular clouds swept out by SNR explosion and shells due to the interaction of the supernova ejecta and the surrounding medium. The experimental data have confirmed the prediction of the discussed models and estimations about the hadronic generation mechanism of very high energy  $\gamma$ -rays in Tycho's SNR, Cas A, IC 443 and  $\gamma$ Cygni SNR. Further deeper investigations in high and very high energies are needed to better constrain on astroparticle acceleration theory and model parameters.





# SHALON observations of Active Galactic Nuclei

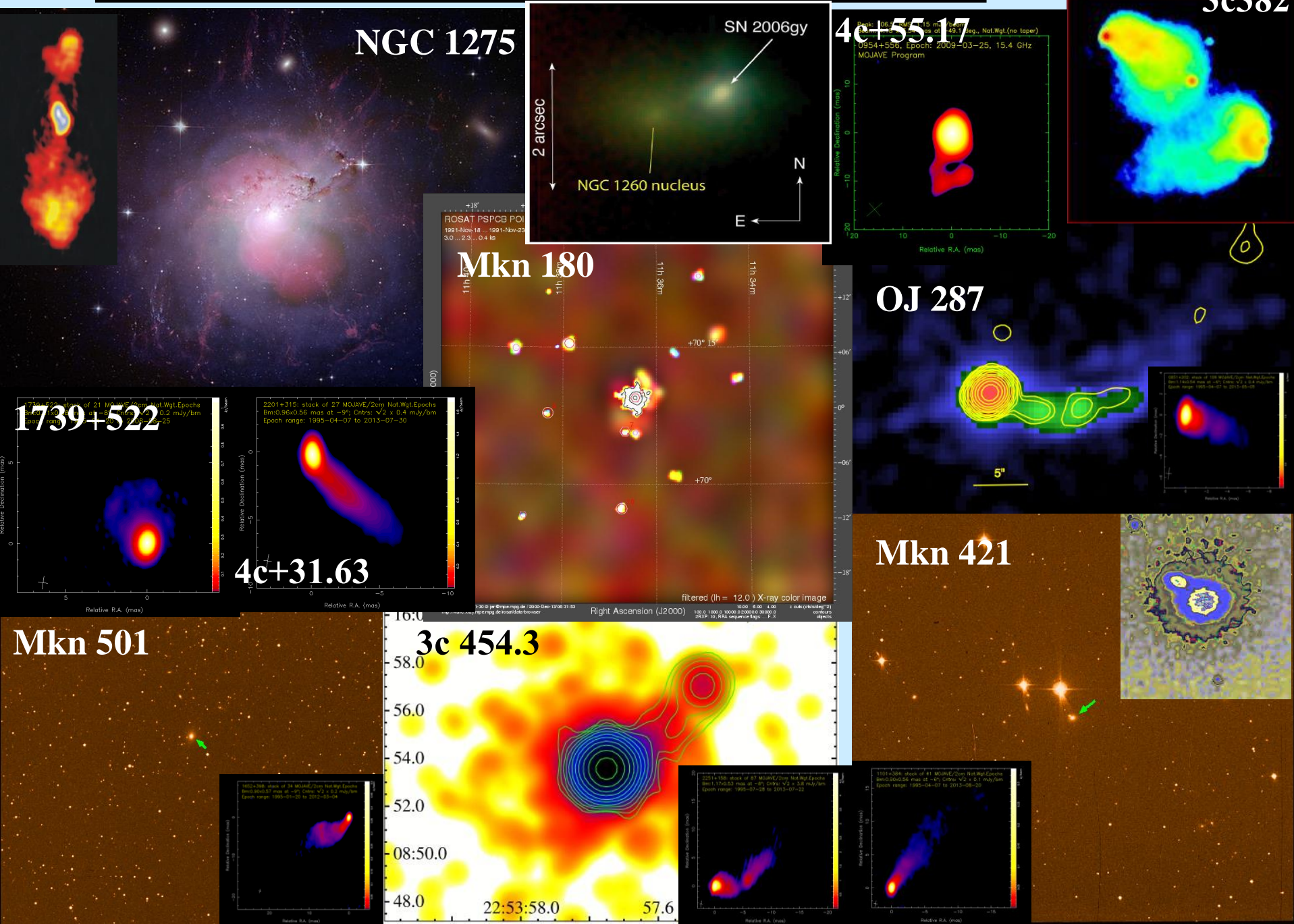


**Table 1.** The catalogue of extragalactic  $\gamma$ -ray sources observed by SHALON with parameters for spectrum fitting in the form of a power law with exponential cutoff  $F(> E) \propto E^{k_\gamma} \times \exp(-E/E_{cutoff})$ .

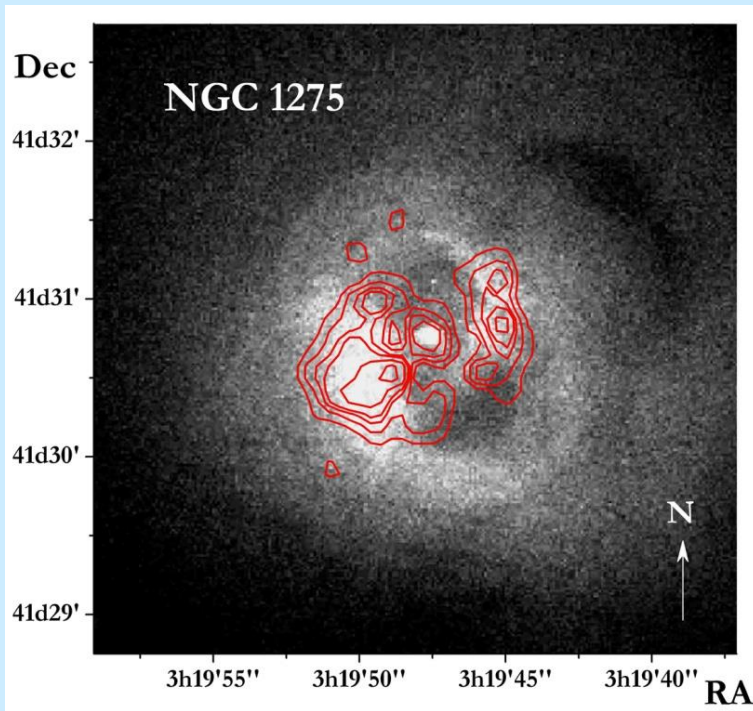
Sources	Observable flux <sup>a</sup>	$k_\gamma$	$E_{cutoff}$ , TeV	Distance, z	Type
NGC 1275	$(0.78 \pm 0.05)$	$-2.18 \pm 0.12$	$32 \pm 7$	0.018	Seyfert
SN2006 gy	$(3.71 \pm 0.65)$	$-3.10 \pm 0.30$	$4.4 \pm 1.9$	0.019	SN
IC 310	$(0.89 \pm 0.09)$	$-0.84 \pm 0.10$	$13 \pm 3.9$	0.019	RG
Mkn 421	$(0.63 \pm 0.05)$	$-1.51 \pm 0.18$	$10 \pm 3$	0.031	BL Lac
Mkn 501	$(0.86 \pm 0.06)$	$-1.48 \pm 0.15$	$11 \pm 3$	0.034	BL Lac
Mkn 180	$(0.65 \pm 0.09)$	$-1.84 \pm 0.15$	$7.3 \pm 2.2$	0.046	BL Lac
3c382	$(0.91 \pm 0.14)$	$-1.05 \pm 0.11$	$21 \pm 7.0$	0.0578	BLRG
4C+31.63	$(0.73 \pm 0.16)$	$-1.13 \pm 0.16$	$10.4 \pm 3.2$	0.295	FSRQ
OJ 287	$(0.26 \pm 0.07)$	$-1.14 \pm 0.11$	$9.5 \pm 1.2$	0.306	BL Lac
3C 454.3	$(0.43 \pm 0.07)$	$-0.52 \pm 0.12$	$6.2 \pm 1.0$	0.859	FSRQ
4C+55.17	$(0.90 \pm 0.16)$	$-1.40 \pm 0.15$	$5.4 \pm 2.1$	0.896	FSRQ
PKS 1441+25	$(0.52 \pm 0.23)$	—	—	0.939	FSRQ
1739+522	$(0.49 \pm 0.05)$	$-0.50 \pm 0.18$	$6.1 \pm 1.2$	1.375	FSRQ
B2 0242+43	$(0.58 \pm 0.20)$	—	—	2.243	FSRQ
B2 0743+25	$(0.37 \pm 0.16)$	—	—	2.979	FSRQ

<sup>a</sup> Integral flux at energy  $> 800$  GeV in units of  $10^{-12} \text{cm}^{-2} \text{s}^{-1}$



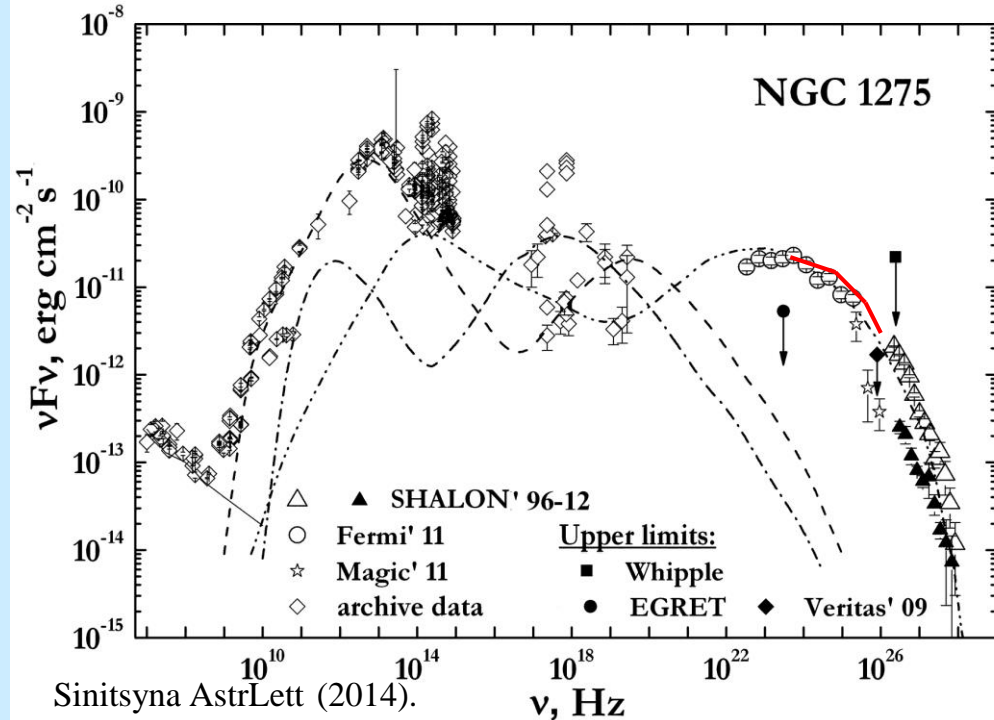


# NGC 1275

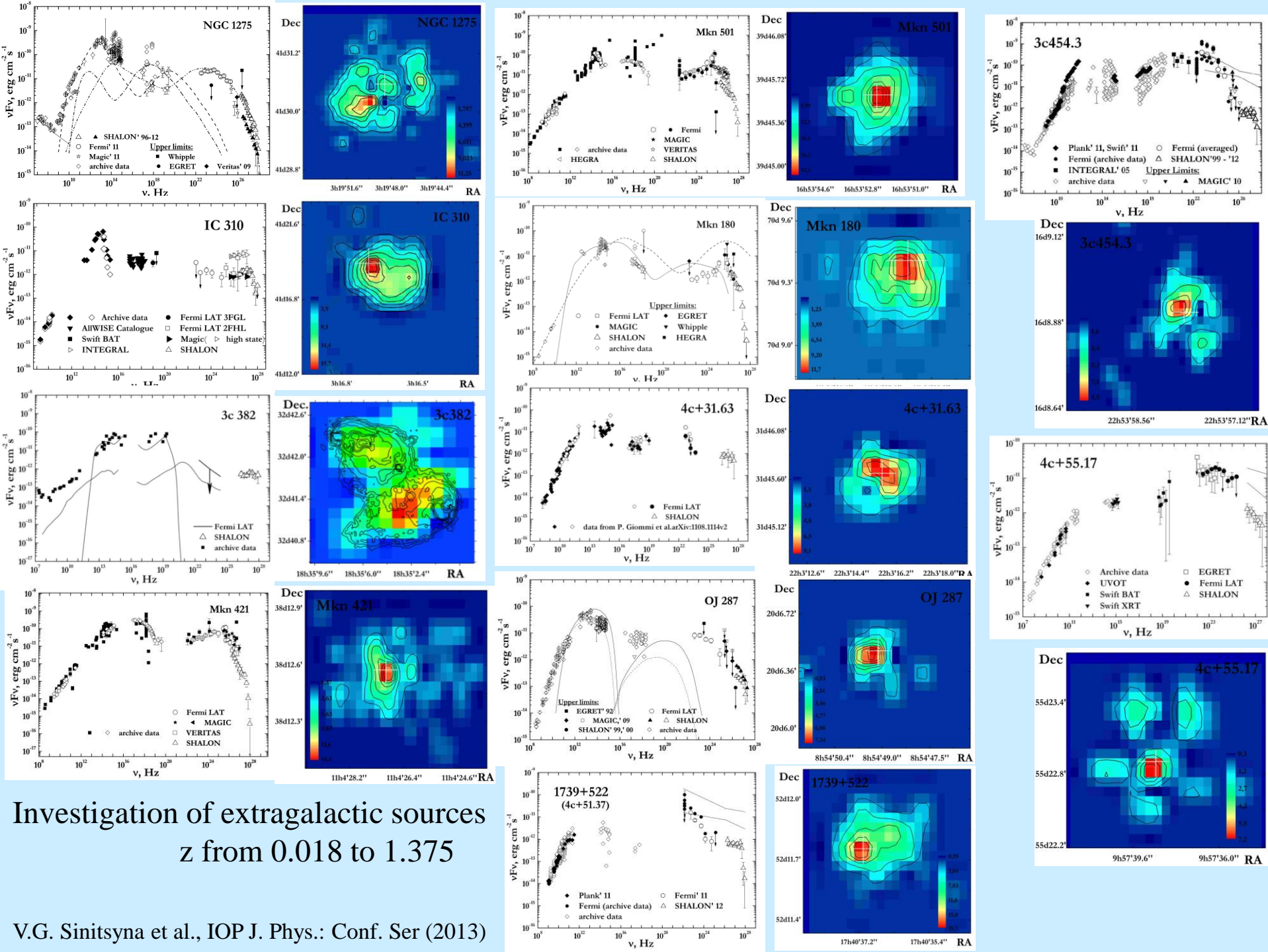


The structures visible in TeV  $\gamma$ -rays are formed through the interaction of very high energy cosmic rays with the gas inside the Perseus cluster and interstellar gas heating at the boundary of the bubbles blown by the central black hole in NGC 1275. The presence of emission in the energy range 1–40 TeV from a central region of  $\sim 32''$  in size around the nucleus of NGC 1275 (black triangles) and the short-time flux variability point to the origin of the very high energy emission as a result of the generation of jets ejected by the central supermassive black hole of NGC 1275.

Long-term studies of the central galaxy in the cluster, NGC 1275, are being carried out in the SHALON experiment. Gamma-ray emission from NGC 1275 was detected by the SHALON telescope at energies 800 GeV - 40 TeV. It was found that the TeV structure around NGC 1275 spatially coincides with the X-ray emission regions. The brightness distribution of the X-ray emission and the observed TeV emission shows a sharp increase in intensity outside the bubbles blown by the central black hole and visible in the radio band. To analyze the emission related to this core, we additionally identified the emission component corresponding to the central region of NGC 1275 with a size of  $32''$ . (Sinitsyna AstrLett2014).



Sinitsyna AstrLett (2014).

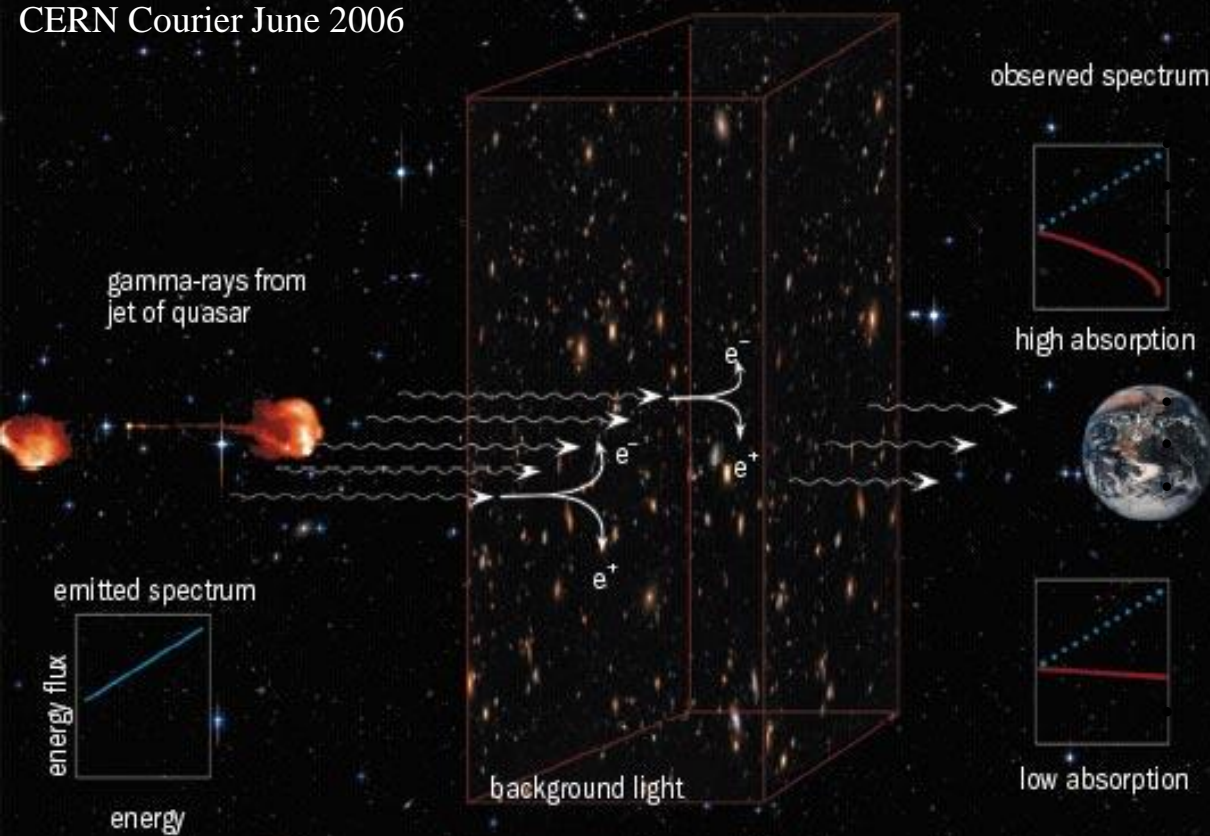




# Metagalactic sources of very high energy gamma-rays

Observations of active galactic nuclei can also be used for the study of Extragalactic Background Light. The light emitted from all objects in the Universe such as stars, galaxies, hot dust etc. during its entire history forms a background light of photons named "diffuse extragalactic background light" (EBL). The EBL spectrum contains an information about star and galaxy formation on early stages of Universe evolution. TeV  $\gamma$ -rays, radiated by distant sources, mostly interact with IR-photon background via  $\gamma + \gamma \rightarrow e^+ + e^-$  resonant process, then relativistic electrons can radiate  $\gamma$ -ray with energies less than of primary  $\gamma$ -quantum. As a result, primary spectrum of  $\gamma$ -source is changed, depending on spectrum of background light. So, a hard spectra of AGNs with high red shifts of 1.6 -1.8 allow to determine an absorption by Extragalactic Background Light and thus spectrum of EBL.

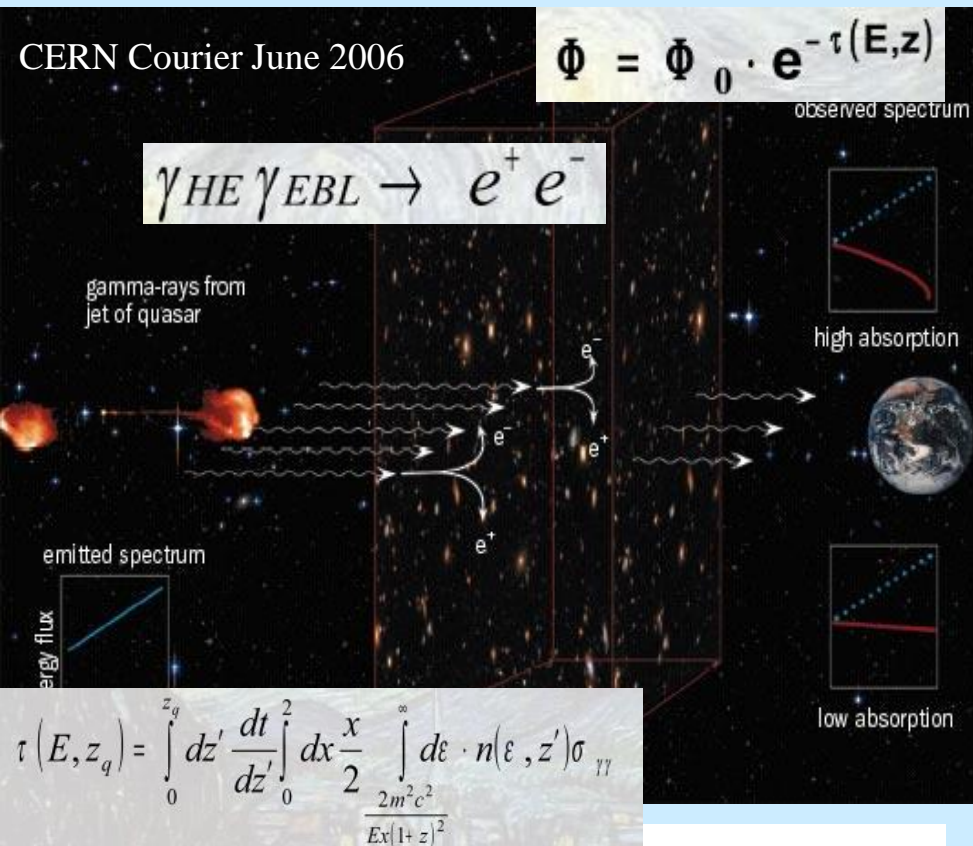
CERN Courier June 2006



During the period 1992-2016 fifteen metagalactic sources have been observed

NGC 1275	$z = 0.0179$ ;
SN 2006gy	$z = 0.019$ ;
IC 310	$z = 0.019$ ;
Mkn 421	$z = 0.031$ ;
Mkn 501	$z = 0.034$ ;
Mkn 180	$z = 0.046$ ;
3c382	$z = 0.0578$ ;
4c+31.63	$z = 0.295$
OJ 287	$z = 0.306$ ;
3c454.3	$z = 0.859$ ;
4c+55.17	$z = 0.896$ ;
PKS 1441+25	$z = 0.939$ ;
1739+522	$z = 1.375$ ;
B2 0242+43	$z = 2.243$ ;
B2 0743+25	$z = 2.949$ ;

Observations of distant metagalactic sources have shown that the Universe is more transparent to very high energy  $\gamma$ -rays than previously believed.



## Extragalactic Background Light

Spectral energy distribution of EBL: measurements and models and EBL shape constrained from observations of the extragalactic sources by SHALON:

- 1 – NGC 1275 ( $z = 0.018$ );  
Mkn 421 ( $z = 0.031$ );  
Mkn 501 ( $z = 0.034$ );  
Mkn 180 ( $z = 0.046$ );  
3c382 ( $z = 0.0578$ );

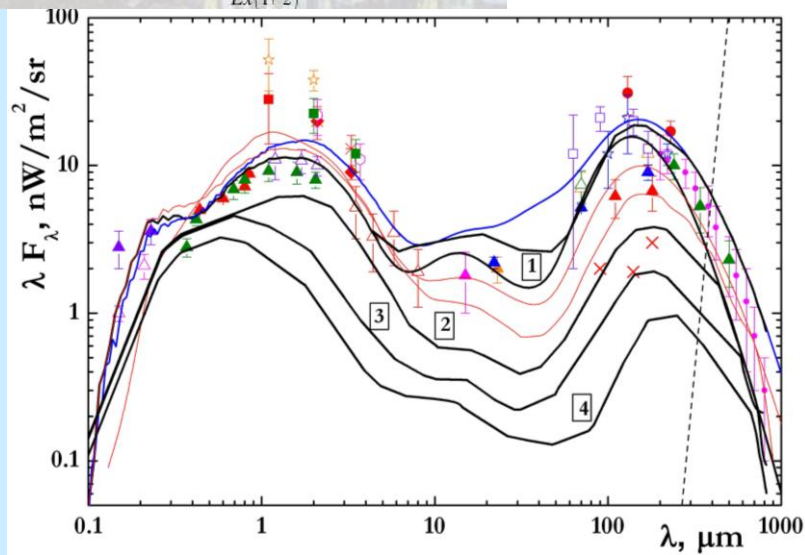
(averaged EBL shape from best-fit model and Low-SFR model)

Upper 1 is for Mkn180 ( $z = 0.046$ )

- 2 – 4c+31.63 ( $z=0.295$ );  
OJ 287 ( $z = 0.306$ );

3 – EBL shape from constrained from observations of 3c454.3 ( $z = 0.859$ );  
4c+55.17( $z = 0.896$ )

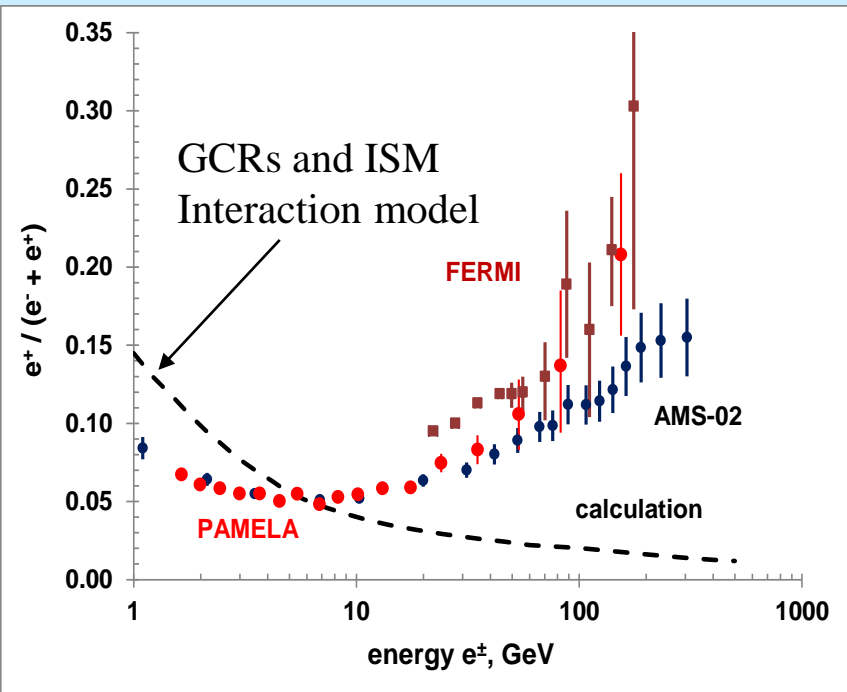
4 – EBL shape from constrained from observations of 1739+522 ( $z = 1.375$ )



V.G. Sinitsyna et al. 2016, IOP J. Phys.: Conf. Ser., 718 052044  
V.G. Sinitsyna, K.A. Balygin, S.S. Borisov, I.A. Ivanov,  
A.M. Kirichenko, A.I. Klimov, I.P. Kozhukhova, R.M. Mirzafatikhov,  
N.I. Moseiko, I.E. Ostashev, V.Y. Sinitsyna 2017, EPJ Web of  
Conferences, v. 145, 19004



# The first detection of TeV gamma-rays from Red Dwarfs



The present point of view on the sources of cosmic rays in Galaxy considers explosions of supernovae as sources of these particles up to energies of  $\sim 10^{17}$  eV. However, the experimental data obtained with Pamela, Fermi, AMS-02, spectrometers requires the existence of nearby sources of cosmic rays at the distances less then 1 kpc from the solar system. These sources could explain such experimental data as the growth of the ratio of galactic positrons to electrons with increase of their energy, the complex dependence of the exponent of the proton and alpha spectra from the energy of these particles, the appearance of anomaly component in cosmic rays.

We consider active dwarf stars as possible sources of galactic cosmic rays in energy range up to  $\sim 10^{14}$  eV. These stars produce powerful stellar flares. The generation of high-energy cosmic rays has to be accompanied by high-energy gamma-ray emission.

Here we present the SHALON long-term observation data aimed to search for gamma-ray emission above 800 GeV from the active red dwarf stars. The data obtained during more than 10 years observations of the dwarf stars V962 Tau, V780 Tau, V388 Cas and V1589 Cyg were analyzed. The high-energy gamma-ray emission in the TeV energy range mostly of flaring type from the sources mentioned above was detected. This result confirms that active dwarf stars are also the sources of high-energy galactic cosmic rays (Stozhkov, 2011).



# V388 Cas



During the observations of Tycho's SNR the SHALON field of view contains V388 Cas as it located at  $\sim 4.5^\circ$  South from Tycho's SNR . So due to the large telescopic field of view ( $\sim 8^\circ$ ) the observations of Tycho's SNR is naturally followed by the observations of V388 Cas flaring star.

SHALON telescope field of view during the observation of Tycho's SNR

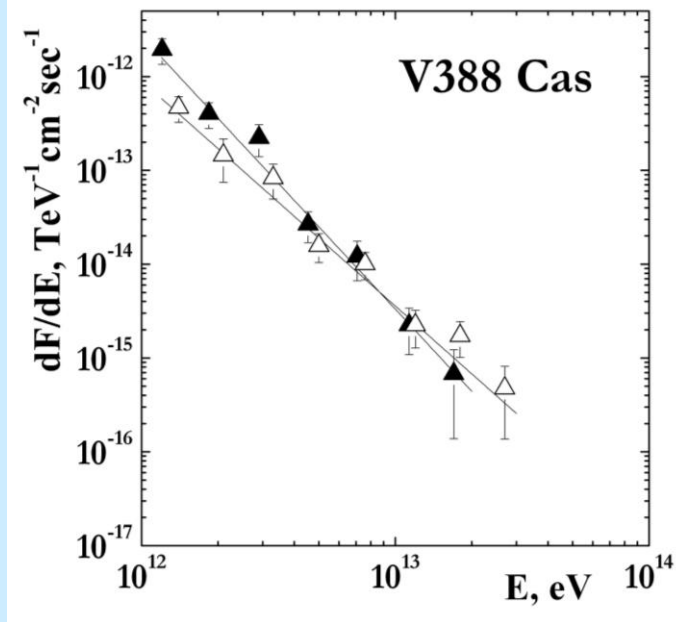
V388 Cas as a source accompanying to Tycho's SNR was observed with SHALON telescope at the period 1996y to 2010y for a total of 93 hours. The  $\gamma$ -ray source associated with the V388 Cas was detected above 1 TeV with a statistical significance  $6.8\sigma$  determined by Li&Ma and with average gamma-ray flux:

$$I_{V388Cas}( > 1 \text{ TeV} ) = (0, 84 \pm 0, 19) \bullet 10^{-12} \text{ cm}^{-2} \text{ s}^{-1}$$

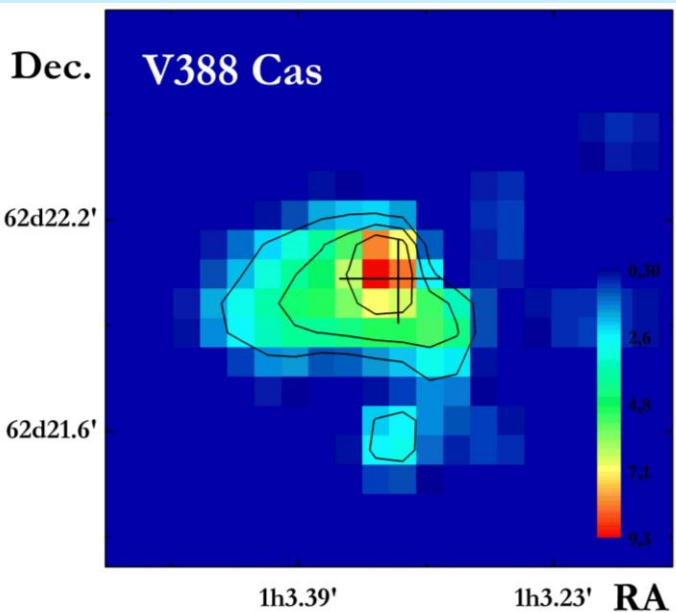
During long-term observation V388 Cas appeared as a source with varying flux and seemed to be detected during the flares.



## V388 Cas



The  $\gamma$ -ray spectra of V388 Cas by SHALON



Emission map of V388 Cas by SHALON

V388 Cas as a source accompanying to Tycho's SNR have been systematically observed with SHALON telescope during the clear moonless nights at zenith angles from  $16^\circ$  to  $35^\circ$ . The observations were performed using the standard for SHALON technique of recording information about the cosmic-ray background and gamma-ray-initiated showers in the same observing session. With the data processing, V388 Cas was detected above 0.8 TeV by SHALON with a statistical significance  $6.8\sigma$  determined by Li&Ma method. The signal significance for this source is much less than one for the source with similar flux and spectrum index obtained in the same observation hours because of less collection field of view relative to the standard procedure of SHALON experiment. After the procession of the Tycho's SNR observation data first by selection criteria associated with Tycho's SNR and then with V388 Cas we found that less 1% of showers are common for the both sources. Recognition of source of each of the common showers is performed by the analysis of angular distance of arrival direction of these showers and source coordinates. This didn't change the average flux of Tycho's SNR.

The shape of SHALON average differential spectrum of gamma rays from V388 Cas in the energy range from 0.8 to 25 TeV fits well to a soft power law :  $dN/dE = (0.91 \pm 0.22) \times 10^{-12} \times (E_\gamma / 1 \text{ TeV})^{-2.52 \pm 0.15}$   
with the  $\chi^2/\text{Dof} = 1.23$  where degree of freedom  $\text{Dof} = 6$   
A flaring spectrum:  $dN/dE_{\text{Flare}} = (2.7 \pm 0.15) \times 10^{-12} \times (E_\gamma / 1 \text{ TeV})^{-2.91 \pm 0.18}$

# V780 Tau and V962 Tau



V780 Tau and V962 Tau flaring stars are in the telescopic field of view during observations of Crab Nebula. V780 Tau is located at the distance of  $\sim 3^\circ$  north from Crab and V962 Tau is of  $2.5^\circ$  east from Crab. As a result, V780 Tau and V962 Tau as a sources accompanying to Crab have been systematically observed with SHALON telescope since 1994 during the clear moonless nights.

SHALON telescope field of view during the observation of Crab Nebula

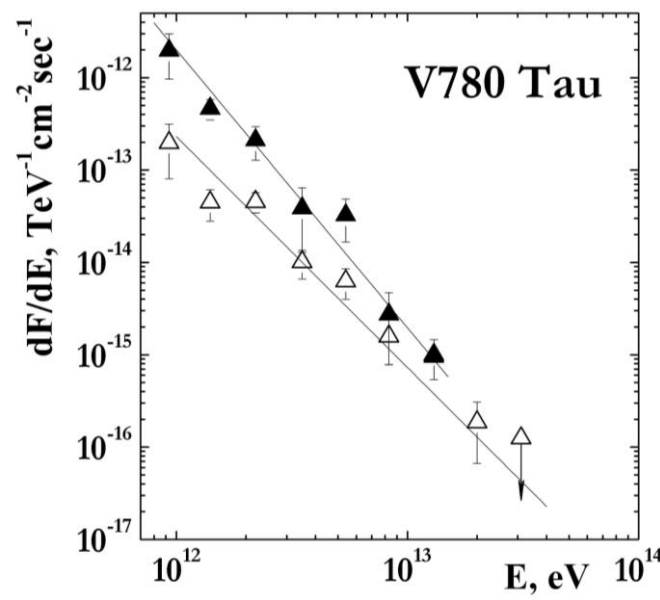
These flaring stars as a source accompanying to Crab were observed with SHALON telescope at the period 1994y to 2014y for a total of 125.2 hours during the clear moonless nights at zenith angles from  $15^\circ$  to  $35^\circ$ . The observations were performed using the standard for SHALON technique of recording information about the cosmic-ray background and gamma-ray-initiated showers in the same observing session. With the data processing, V780 Tau and V962 Tau were detected above 0.8 TeV by SHALON with the average integral flux :

$$I_{V780\text{Tau}}(>1\text{TeV}) = (0,23 \pm 0,03) \bullet 10^{-12} \text{ cm}^{-2}\text{s}^{-1}$$

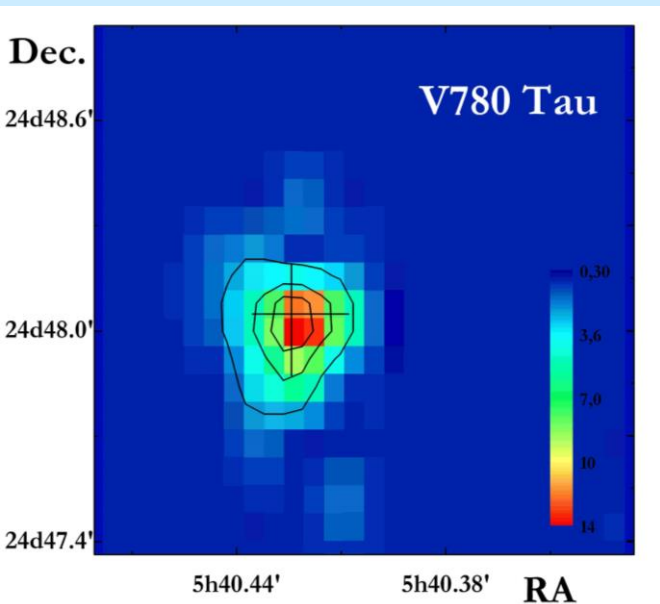
$$I_{V962\text{Tau}}(>1\text{TeV}) = (0,39 \pm 0,04) \bullet 10^{-12} \text{ cm}^{-2}\text{s}^{-1}$$



# V780 Tau



The  $\gamma$ -ray spectra of V780 Tau by SHALON



Emission map of V780 Tau by SHALON

V780 Tau was detected above 0.8 TeV by SHALON with a statistical significance  $6,1\sigma$  determined by Li&Ma method. The signal significance for this source is also much less than one for the source with similar flux obtained in the same observation hours because of less collection field of view relative to the standard experiment procedure. After the procession of the Crab observation data first by selection criteria associated with Crab and then with V780 Tau we found that less than 1% of showers are common for the both sources. Recognition of source of each of the common showers is performed by the analysis of angular distance of arrival direction of these showers and source coordinates. As a result, less than  $\sim 0,4\%$  of Crab showers were recognized to be V780 Tau showers. This didn't change the average flux of Crab.

In observations since 1994y V780 Tau was found to be varying. The flaring spectrum was also extracting (▲).

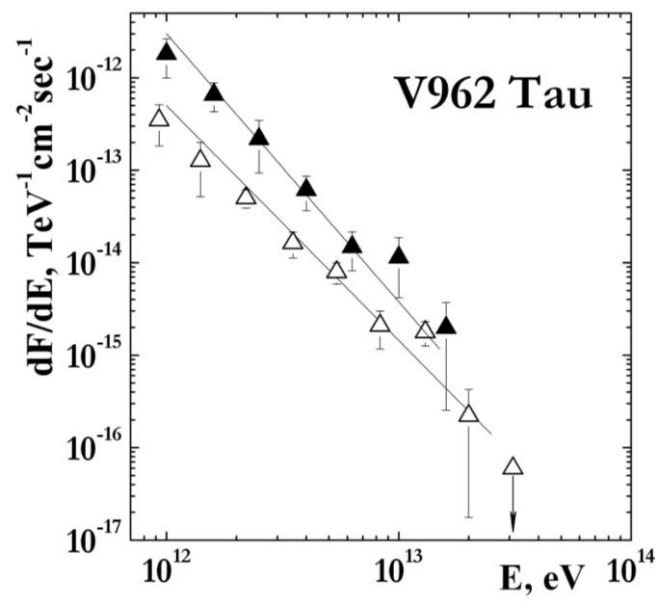
The shape of SHALON differential spectrum of gamma rays from V780 Tau in the energy range from 0.8 to 20 TeV fits well to a hard power law with an exponential cutoff:

$$dN/dE = (0,21 \pm 0,08) \times 10^{-12} \times (E_{\gamma}/1 \text{ TeV})^{-2,51 \pm 0,15}$$

with the  $\chi^2/\text{Dof} = 1,31$  where degree of freedom  $\text{Dof} = 5$

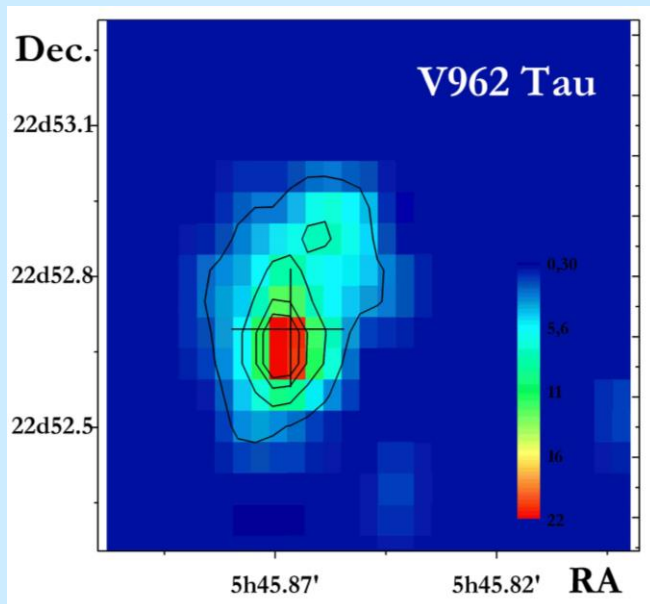
A flaring spectrum:  $dN/dE_{\text{Flare}} = (2,0 \pm 0,15) \times 10^{-12} \times (E_{\gamma}/1 \text{ TeV})^{-3,01 \pm 0,21}$

# V962 Tau



The  $\gamma$ -ray spectra of V962 Tau by SHALON

V962 Tau was detected above 0.8 TeV by SHALON with a statistical significance  $7,7\sigma$  determined by Li&Ma method. The signal significance for this source is also less than one for the source with similar flux obtained in the same observation hours because of less collection field of view relative to the standard experiment procedure. After the procession of the Crab observation data first by selection criteria associated with Crab and then with V780 Tau we found that there are no showers common for the both sources.



Emission map of V962 Tau by SHALON

V962 Tau was also found to be varying. The flaring spectrum is presented with  $\blacktriangle$ .

The differential spectrum of gamma rays from V962 Tau in the energy range from 0.8 to 20 TeV fits well to a power law :

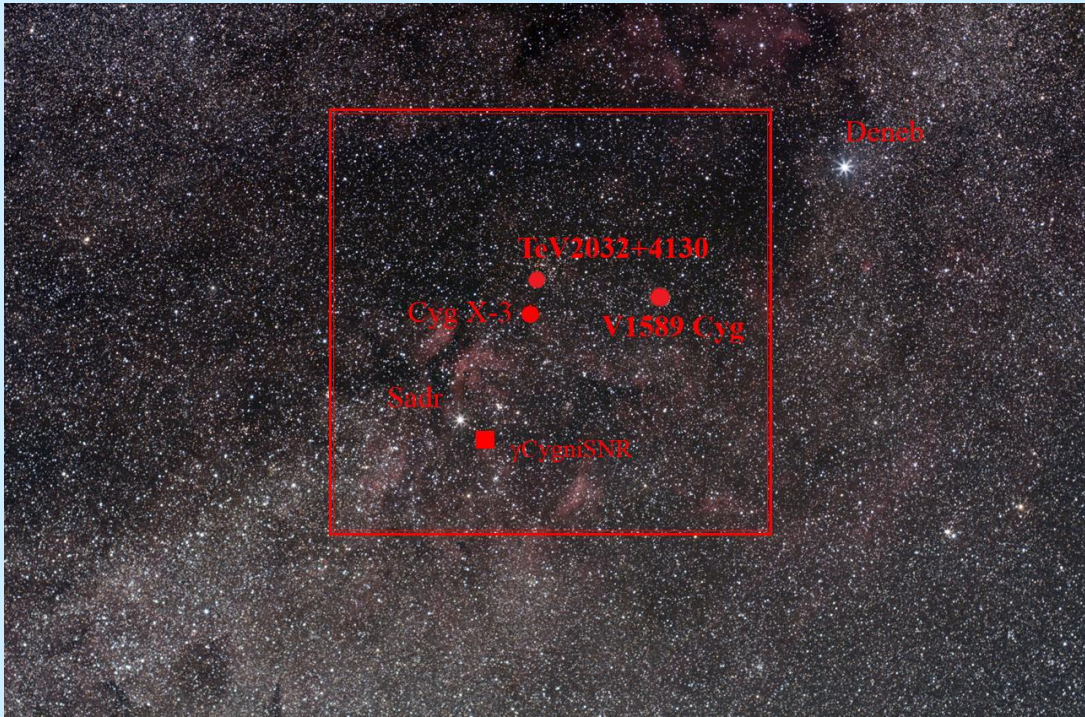
$$dN/dE = (0,40 \pm 0,17) \times 10^{-12} \times (E_{\gamma}/1 \text{ TeV})^{-2,54 \pm 0,15}$$

with the  $\chi^2/\text{Dof} = 0,87$  where degree of freedom  $\text{Dof} = 6$

A flaring spectrum:  $dN/dE_{\text{Flare}} = (2,8 \pm 0,45) \times 10^{-12} \times (E_{\gamma}/1 \text{ TeV})^{-2,95 \pm 0,22}$



# V1589 Cyg



V1589 Cyg is located at the distance of  $\sim 2^\circ$  west from Cyg X-3. So due to the large telescopic field of view  $> 8^\circ$  the observations of Cygnus-X are naturally followed by the tracing of V1589 Cyg. As a result, V1589 Cyg as a source accompanying to Cyg X-3 have been systematically observed with SHALON telescope (since 1995 up to 2016) during the clear moonless nights at zenith angles from  $5^\circ$  to  $34^\circ$  for a total of 303.5 hours .

SHALON telescope field of view during the observation of Cyg X-3

In accordance with the program on long-term studies of microquasar Cygnus X-3 at very high energies, observations of Cygnus Region and its objects, including V1589 Cyg, as well as TeV J2032+4130 and  $\gamma$ Cygni SNR are being carried out with SHALON.

With the data processing, V1589 Cyg was detected above 0.8 TeV by SHALON with the average integral flux :

$$I_{V1589Cyg}( > 0,8 \text{ TeV} ) = (0,13 \pm 0,019) \bullet 10^{-12} \text{ cm}^{-2} \text{ s}^{-1}$$

# V1589 Cyg

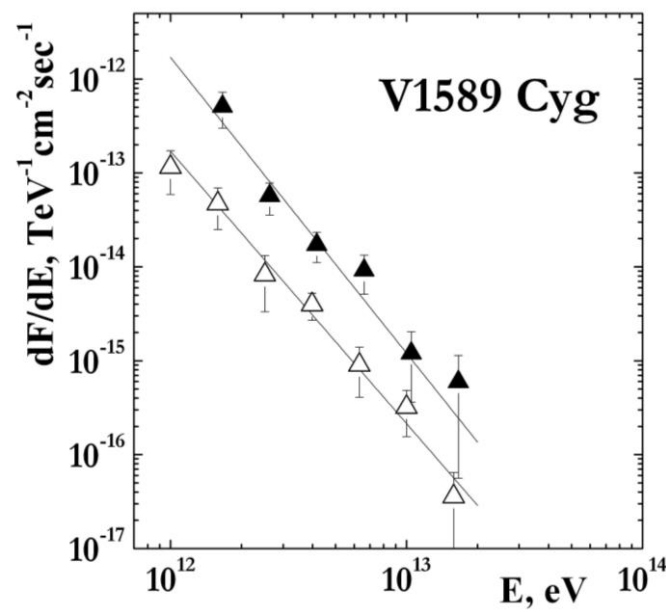
V1589 Cyg as a source accompanying to Cyg X-3 have been systematically observed with SHALON. The observations were performed using the standard for SHALON technique of recording information about the cosmic-ray background and gamma-ray-initiated showers in the same observing session. With the data processing, V1589 Cyg was detected above 0.8 TeV by SHALON with a statistical significance  $6.5\sigma$  determined by Li&Ma method. The signal significance for this source is less than one for the source with similar flux and spectrum index obtained in the same observation hours because of less collection field of view relative to the standard procedure of SHALON experiment. The corrections for the effective field of view were made. After the procession of the Cyg X-3 observation data first by selection criteria associated with Cyg X-3 and then with V1589 Cyg we found that less than 2% of showers are common for the both sources. Recognition of source of each of the common showers is performed by the analysis of angular distance of arrival direction of these showers and source coordinates. As a result, less than 1% of Cyg X-3 showers were recognized to be V1589 Cyg showers. This didn't change the average flux of Cyg X-3. During long-term observation V1589 Cyg appeared as a source with varying flux. The flaring spectrum was also extracting and presented with ▲.

The shape of SHALON differential spectrum of gamma-rays from V1589 Cyg in the energy range from 0.8 to 35 TeV fits well to a soft power law:

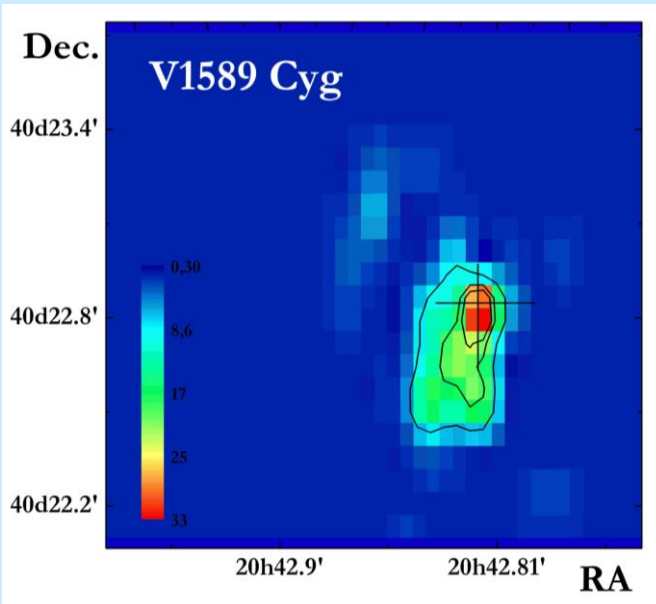
$$dN/dE = (0,15 \pm 0,05) \times 10^{-13} \times (E_{\gamma}/1 \text{ TeV})^{-2,91 \pm 0,18}$$

with the  $\chi^2/\text{Dof} = 0,89$  where degree of freedom  $\text{Dof} = 5$

A flaring spectrum:  $dN/dE_{\text{Flare}} = (1,7 \pm 0,45) \times 10^{-12} \times (E_{\gamma}/1 \text{ TeV})^{-3,15 \pm 0,29}$



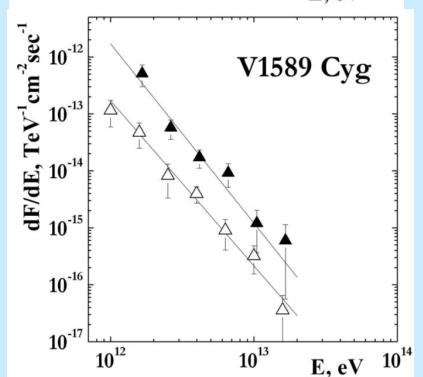
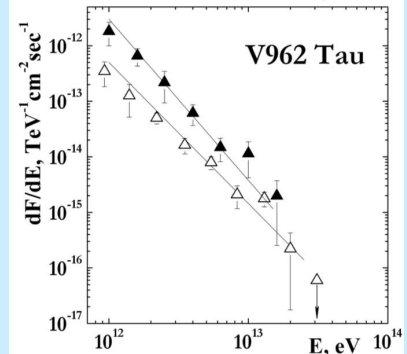
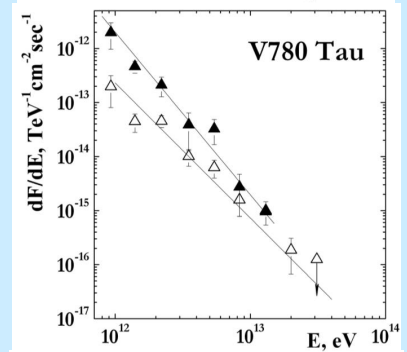
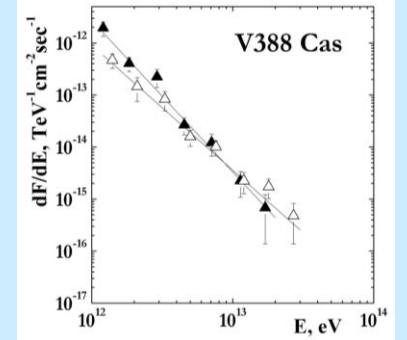
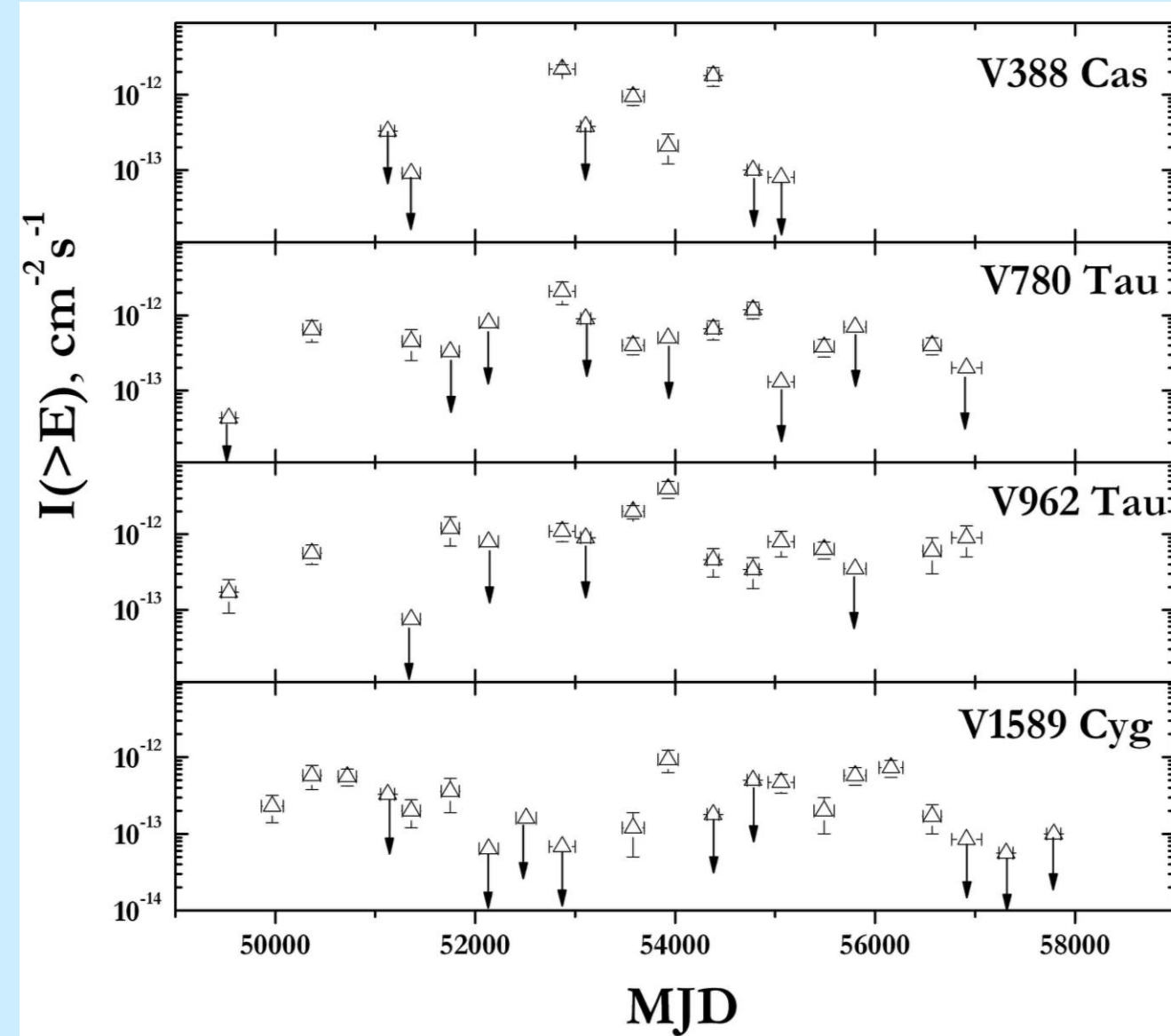
The  $\gamma$ -ray spectra of V1589 Cyg by SHALON



Emission map of V1589 Cyg by SHALON

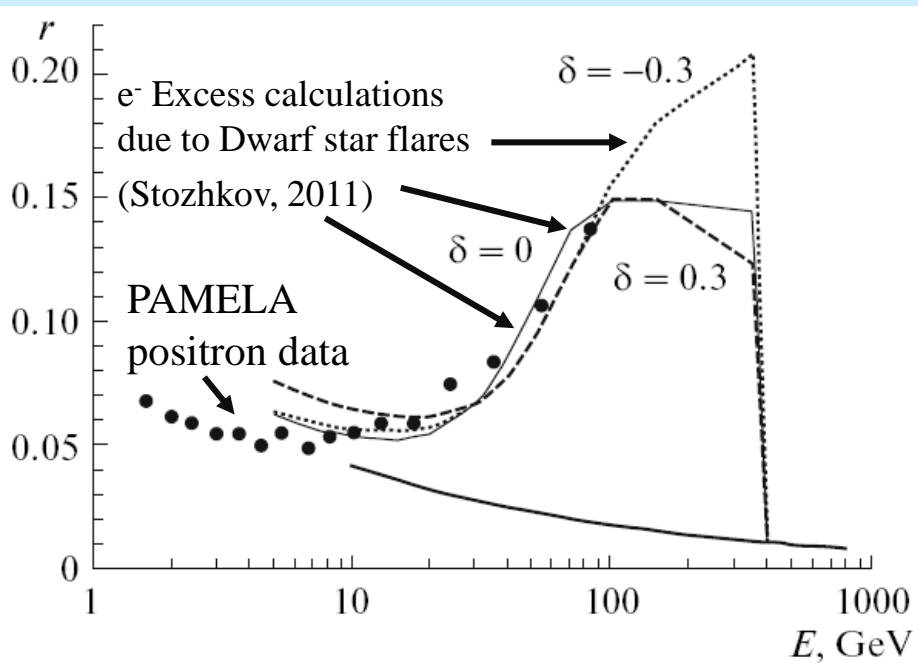


# Light curves of V388 Cas, V780Tau, V962 Tau and V1589 Cyg



The light curves of V388 Cas, V780Tau, V962 Tau and V1589 Cyg and their energy spectra at TeV energies obtained in the long-term SHALON observations.

# GCRs from M-Dwarf star flares



M-Dwarf stars are characterized by flaring events which occur frequently with flare duration varies in time but total duration of  $>10^4$ s. Very high energy gamma-ray fluxes presented here demonstrate that these objects produce the flares of  $\sim 10^{33} - 10^{35}$  ergs.

The energy released in a stellar flares and its frequency are able to provide the necessary energy of GCRs in the disk of our Galaxy and make a significant contribution to the GCR spectrum up to energies of  $E \sim 10^{13} - 10^{14}$  eV (Stozhkov, 2011). The urgent point is that the sources of GCRs are placed at the distances less then 1 kpc from the solar system. Then some of these accelerated GCR escape into the interstellar medium and then interact. An source of positrons is the decay of neutral pions into two gamma-rays and the subsequent formation of  $e^+ e^-$  pairs by these gamma rays.

Positrons and electrons from stellar flares with  $E > 5$  GeV escape into the interstellar medium from a flare region with strong magnetic fields. Thus, there is an additional source of  $e^+$  that explains the anomalous PAMELA effect. It should be noted that most of the electrons (and protons) are accelerated during the stellar flare and the addition of another  $e^-$  flux via the mechanisms of  $\pi^0$  and  $\pi^-$  decays constitutes only a small part of the main flux. The additional source of  $e^+$ , however, provides the main flux of these particles in the Galaxy up to energies of  $E \approx (300-400)$  GeV (see calculations in Stozhkov, Bull. RAS, 75(3), p323, 2011).



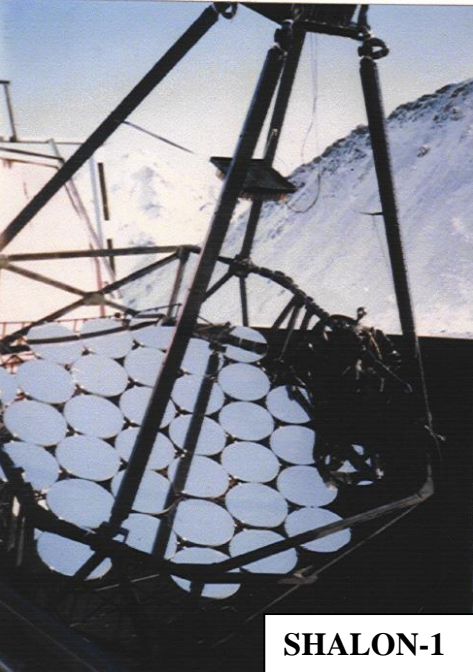


## Conclusion

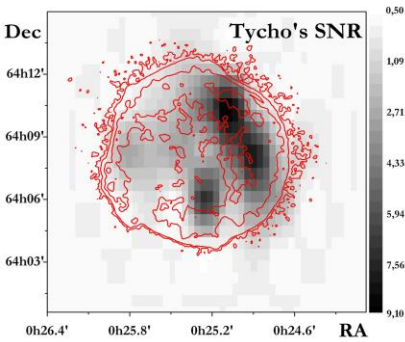
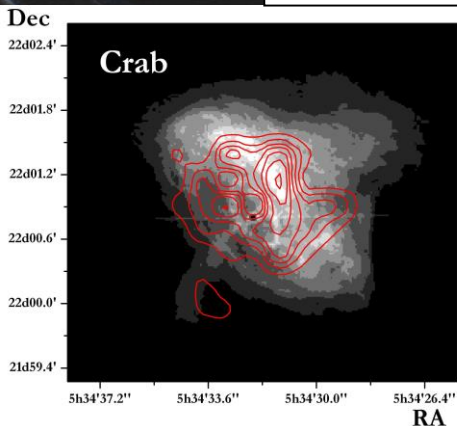
SHALON are the imaging atmospheric Cherenkov telescopes creating in the P.N.Lebedev Physical Institute for gamma-ray astronomy at the energies of 800 GeV to 100 TeV. The idea of enhancement of angular resolution and sensitivity to the  $\gamma$ -rays with construction of the wide field of view was realized in SHALON telescopes since the construction.

SHALON experiment aimed on 800 GeV – 100 TeV gamma-astronomy has been successfully operating since 1992 and covers the wide astroparticle physics topics including an acceleration and origin of cosmic rays in supernova remnants, the physics of relativistic flaring objects like a black holes and active galactic nuclei as well as the long-term studies of the different type objects. The high-energy gamma-ray emission in the TeV energy range mostly of flaring type from the red dwarf stars was detected. This result confirms that active dwarf stars are also the sources of high-energy galactic cosmic rays and can give a base for explanation of GeV "positron excess" phenomena.

- Further deeper investigations in high and very high energies are needed for the better understanding on astroparticle VHE phenomena in Universe.



SHALON-1



SHALON-2

